BRAIN-MACHINE-MUSCLE INTERFACES FOR RESTORING LOCOMOTION AFTER SPINAL CORD INJURIES

ALAM MD. MONZURUL

Ph.D

The Hong Kong Polytechnic University

2013

The Hong Kong Polytechnic University

Department of Rehabilitation Sciences

Brain-machine-muscle interfaces for restoring locomotion after spinal cord injuries

Md. Monzurul Alam

A thesis submitted in partial fulfillment of the requirements of the Degree of Doctor of Philosophy

July 2013

CERTIFICATE OF ORIGINALITY

I hereby declare that this thesis is my own work and that, to the best of my knowledge and belief, it reproduces no material previously published or written, nor material that has been accepted for the award of any other degree or diploma, except where due acknowledgement has been made in the text.

_____ (Signed)

Md. Monzurul Alam (Name of Student)

To my beloved daughter, Megha Anjum.

ABSTRACT

Spinal Cord Injury (SCI) is a devastating neuronal dysfunction affecting a large population worldwide. Regaining lower-limb functionality such as walking is one of the highest priorities among all the disabilities of SCI paraplegics. Although the ultimate recovery would be repairing or regenerating new axons across the injured lesion potentially by stem cells or other transplants and neurotropic factors, long standing challenges to achieve this as well as recent technological advancements demand the development of neuroprosthetic devices to restore motor function following the injury.

Brain-machine interface (BMI) is a neuroprosthetic approach for restoring motor function in paralysed patients. While BMI neuroprostheses have been successfully evaluated for restoring upper-limb functions, very little research has focused on developing such systems to restore lower-limb functions. This research study addresses the following questions: 1) whether different step gait-related neural information can be captured in parallel from rats' primary motor cortex during walking, and 2) whether and how this neural information can be utilized to restore locomotion after complete spinal transections.

In the current study, spinal rats (mid-thoracic transection) were utilized as the animal model to design and develop a hindlimb BMI for locomotion. Neural signals recording were accomplished from the hindlimb area of the primary motor cortex (M1) to decode the "*intent*" of locomotive information during treadmill walking. The results show a strong association of neural activities with step gait cycles in healthy subjects. These neural activities dropped significantly following spinal transection. However, the locomotive states (standing or walking) could still be successfully decoded from these neural recordings. Finally, a novel BMI device was developed

that processes this real-time neural information to electrically activate paralysed hindlimb muscles to mimic stepping.

This study proposes lower-limb BMI as a future neuroprosthesis for SCI paraplegics.

Key-words: Brain-machine interface, spinal cord injury, locomotion, neural signals recording, functional electrical stimulation, neuroprosthetics.

PUBLICATION ARISING FROM THE THESIS

Journal publications

Monzurul Alam, Xi Chen, Zicong Zhang, Yan Li and Jufang He (2013), "A brain-machine-muscle interface for restoring hindlimb locomotion after complete spinal transection in rats". (Submitted to Frontiers in Neuroscience)

Yan Li, **Monzurul Alam**, Shanshan Guo, K.H. Ting, and Jufang He (2013). "Electronic bypass of spinal lesions to activate lower motor neurons directly driven by cortical neural signals". (Submitted to Journal of Neuroengineering and Rehabilitation)

Book chapter publication

Monzurul Alam and Jufang He (2013), "Lower-limb Neuroprostheses: Restoring walking after spinal cord injury". (Submitted as a chapter in the Book: Emerging Theory and Practice in Neuroprosthetics; Publisher: IGI-Global)

Peer reviewed conference proceeding

Monzurul Alam and Jufang He, "Cortically Controlled Electrical Stimulation for Locomotion of the Spinal Cord Injured" In *Converging Clinical and Engineering Research on Neurorehabilitation.Volume* 1. Edited by Pons JL, Torricelli D, Pajaro M: Springer Berlin Heidelberg; 2013: 35-40:*Biosystems & Biorobotics*.

ACKNOLEDGEMENTS

I like to express my deepest gratitude to my chief supervisor, Prof. Jufang He, whose worthy guidance, stimulating suggestions, motivations and encouragements from the first day of my study enabled me to accomplish this project. I am also very grateful to my co-supervisor, Dr. Stephanie Au-Yeung for her valuable suggestions, encouragements and supports throughout the research study.

It is my great pleasure to thank those who made this thesis possible, especially to mention Dr. Xi Chen, Dr. Yiping Guo, Mr. Zicong Zang and other colleagues in the lab.

Especially, I like to thank my family for their support to me to stay in focus on the research and achieving this work.

I also like to express my heartfelt appreciation to Mr. & Mrs. P. K. Yu Memorial Scholarship for supporting the research study.

CONTENTS

CHAPTER 1: INTRODUCTION

Spinal cord injury

Spinal Cord Injury (SCI) is a devastating neural dysfunction presumably affecting a large population worldwide. Though the exact prevalence of SCI is unknown (Wyndaele and Wyndaele, 2006), according to the most recent statistics (Cripps et al., 2011), it is estimated that the number of injuries are between 236 and 1,009 per million suggesting 1.65 to 7.06 million worldwide (considering the current world population of approximately 7 billion). The incidence rate, measured globally (23 cases per million or 179,312 cases per annum) is also very high making it one of the top paralyzing medical conditions (Lee et al., 2013). Unfortunately even now the incidences of SCI are not registered in most countries but only some (Noonan et al., 2012). In the United States about 20,000 new injuries occur every year (Bernhard et al., 2005), while in China this number is much larger, standing at over 60,000 new injuries each year (Qiu, 2009). In contrast, in Australia, it is estimated that currently 10,000 people are living with spinal cord injuries (O'Connor, 2004), with 350-400 new cases each year (NeuRA, 2009).

According to the world report on disability (WHO, 2011), the average life-time cost for SCI is estimated to be between $5 million to $9.5 million per incidence. At the same time, other reports estimate that in the United States the life-time cost can reach $3 million, and the annual medical cost ranges from $15,000 to $30,000 per year (French et al., 2007; CDC, 2010). In contrast, the total life time costs of SCI patients are very high in Australia, estimated at $2 billion (AUS) per year (SIA, 2010).

Traumatic SCI usually occurs due to a contusion of the spinal cord resulting from a fracture or dislocated vertebra (SCI-recovery, 2013). The injuries are mainly

from motor vehicle accidents, falls, sports and work-related injuries, war, and violence like stab or gunshots etc. (Bogdanov, 2010). However, SCI may also occur due to non-traumatic causes such as cancer, infection, intervertebral disc disease etc. (van den Berg et al., 2010). While traffic accidents are the leading cause of SCI in developed countries, falls are the leading cause in developing countries (Chiu et al., 2009). SCI injuries are higher in males in all countries; men are injured over four times more than the women (Branco et al., 2007). The average age of these injured is around 35 years, making it an even more devastating medical condition for the rest of their life (Jackson et al., 2004).

Paralysis following SCI can partially or even completely disrupt neural communications between the brain and body resulting in disability regarding movements and sensations. Some sensory-motor functions may remain after incomplete injuries, and possibly be improved by extensive physical rehabilitation; however, in complete injuries generally no sensory-motor functions are left and rarely can be restored (Crozier et al., 1991; Waters et al., 1991).

In 1982, the American Spinal Cord Injury Association (ASIA) published the first edition of the International Standards of Neurological Classification of Spinal Cord Injury (ISNCSCI). Now-a-days, the ISNCSCI (6^{th} edition) is widely used to identify motor and sensory impairment following spinal cord injuries. According to the neurological assessment of the ISNCSCI, ten key muscles and key sensory points of touch and pinprick are tested in each dermatome on the each side of body (Thuret et al., 2006). A complete classification of SCI is illustrated in Figure 1.1.

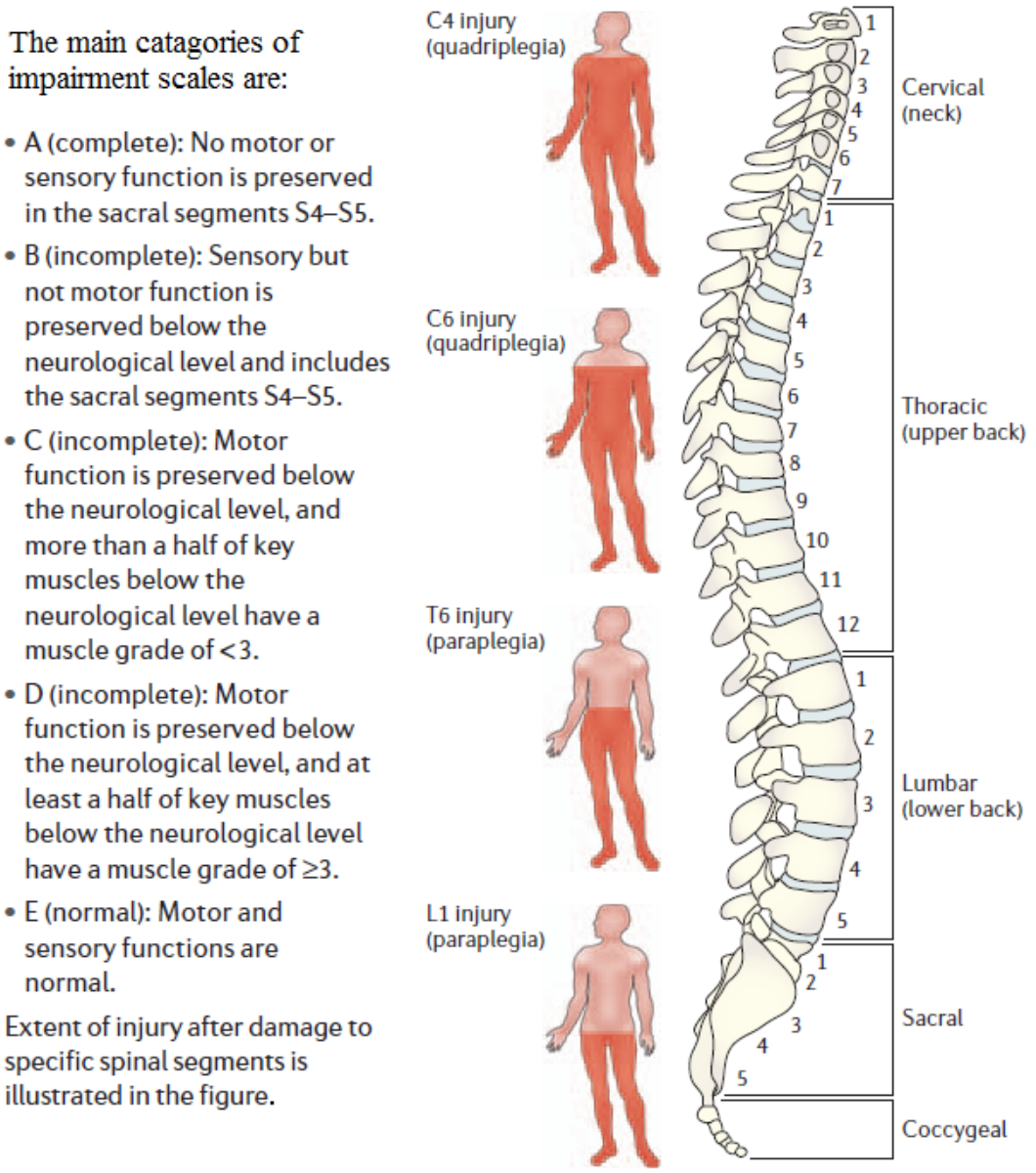

Figure 1.1 Classification of SCI severity using the American Spinal Injury Association (ASIA) impairment scale (reprinted with permission from Thuret et al., 2006)

According to the statistics, among all spinal cord injuries roughly 52% of patients are paraplegics, i.e. no or less sensory-motor function in the lower-limbs (Matthew, 2002). It is also found that these patients desire restoration of walking as one of their top priorities among all the other complications, such as temperature regulation, bladder and bowel control etc. (Anderson, 2004). Hence, it is very

important to find the solution to restore walking in these SCI paraplegics. In this thesis I focus on the current and future therapeutic efforts in relation to restoration of lower-limb motor functions for SCI paraplegics.

Current treatments for SCI paraplegics

Currently, there is no complete cure for SCI injuries (Thuret et al., 2006). However, physical rehabilitation following SCI aims to restore sensory-motor functions of individuals so that they are able to become independent in their daily activities. There are two main strategies to accomplish this: one is functional recovery and the other comprises compensatory strategies. These strategies are used during an individual's rehabilitation program. The recovery strategies are dependent on several factors including severity of the injury, level of the lesion, resources availability, level of family and community support, and clinical practice guidelines developed by physiotherapists and physicians. In cases of severe or complete paraplegia, daily activities like transferring body weight from one place to another (such as from bed to wheelchair or car) are typically accomplished using compensatory strategies, such as focusing on strengthening and utilizing unaffected arms and hands. Less severe or incomplete injuries offer greater chances of recovery of functions, thereby warranting the use of functional recovery strategies (Harkema et al., 2012).

In Recent years, activity-based therapy has been used as evidence-based medicine in physical rehabilitation to activate the neuromuscular system below the level of lesion of the spinal cord (Dromerick et al., 2006; Sadowsky and McDonald, 2009; Harkema et al., 2012). Task-specific rehabilitation is mainly emphasized when the target is to acquire greatest possible extent of recovery without compensation during treatment. Activity dependent plasticity is achieved by providing repetitive

sensory inputs to the spinal circuitry during the training. This aims to retrain the nervous system to recover a specific motor task, such as walking. This training intrinsically activates the injured nervous system with sensory and proprioceptive inputs with less or weak supraspinal controls. Though this method is quite successful in motor incomplete SCI patients, it largely fails to restore any function in motor complete SCI patients (Behrman and Harkema, 2007; Harkema et al., 2012). However, a recent groundbreaking study on a clinically complete paraplegic man has demonstrated that the nervous system can also be extrinsically activated by providing electrical stimulation to lower motor neurons to restore standing and stepping even in the absence of supraspinal inputs (Harkema et al., 2011).

Functional electrical stimulation

Neuromuscular stimulation

In 1960, Kantrowitz was the first to demonstrate the standing of a paraplegic patient by simultaneous electrical stimulation of the quadriceps muscles (Kantrowitz, 1960). This functional restoration of standing influenced many researchers worldwide to investigate and develop further methods to restore lost motor functions following SCI. A Functional Electrical Stimulation (FES) system ideally restores difference motor functions, such as standing, walking, transferring body-weight, reaching etc., though the definition is rather loose, and more practical augmentation of such motor functions. The approaches taken by lower-limb FES systems are broadly categorized into three: surface FES systems, percutaneous and implanted FES systems and hybrid FES systems.

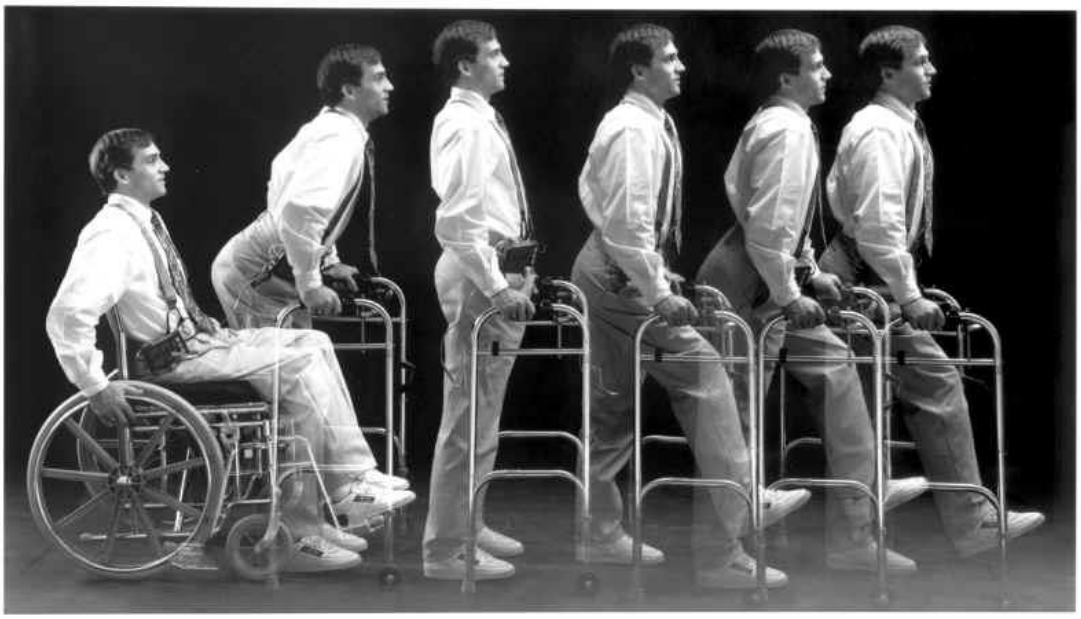

Figure 1.2 The Parastep® system (reprinted with permission from Graupe, 2008)

Surface FES systems

For more than 30 years, surface FES systems have been used in rehabilitation for SCI patients. The first surface FES system was developed in 1970, when two Slovenian scientists, Kralj and Bajd demonstrated that stimulation of the peroneal nerve generated reflex withdrawal with flexion of the hip, knee and ankle joints which simulates the swing phase of walking (Kralj and Grobelnik, 1973; Krajl et al., 1986). This was combined with previously learned quadriceps stimulation to reanimate the swing and stance phases of walking, and a manually controlled surface FES system called Parastep® (as shown in Figure 1.2) was designed and developed in 1982 (Graupe, 2008). The Parstep® system received United States Food and Drug Administration (FDA) approval in 1994 (Chaplin, 1996). To date, approximately 1,000 complete paraplegics are or have been able to ambulate over short distances using the Parstep® system and showed positive responses (Graupe, 2008; Braz et al., 2009). However, high current consumptions for surface electrical stimulation, the low special resolution of stimulation, and stimulation generated fatigues were the

main concerns of surface-based FES systems that lead the investigators to design power efficient, more selective and deep muscle stimulation FES systems.

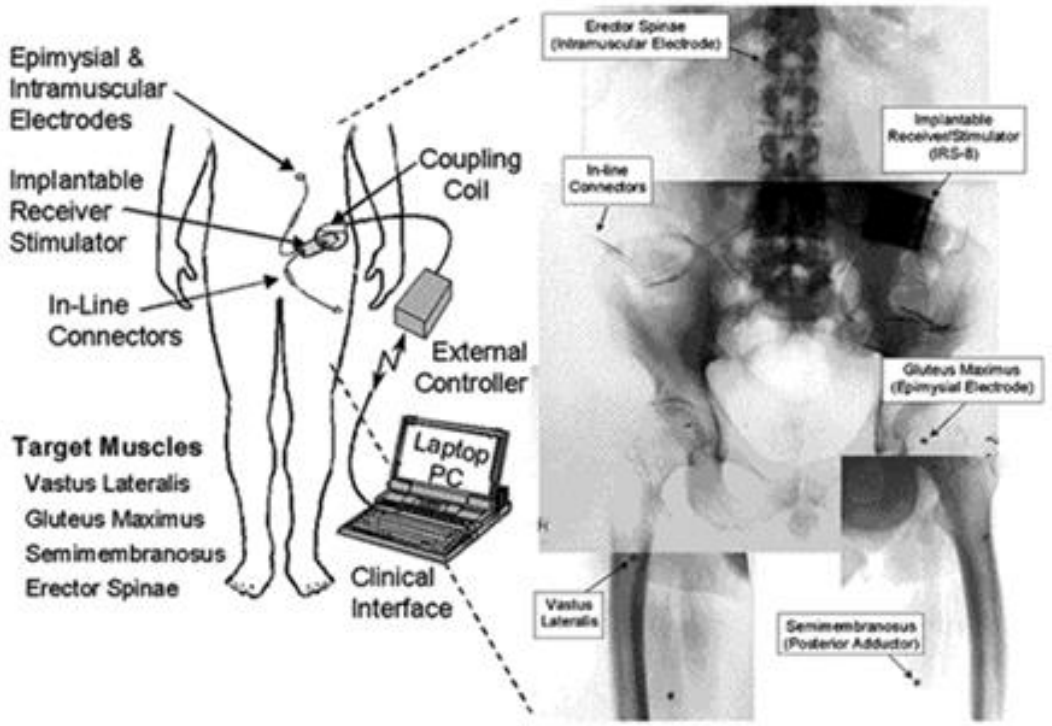

Figure 1.3 VA/CWRU Standing System (reprinted with permission from Agarwal et al., 2003)

Percutaneous and implanted FES systems

Implantable FES systems utilize percutaneous stimulation electrodes to activate deep muscles for more complex lower limb movements compared to their counterpart surface FES systems. Though as many as 48 individual muscles can be activated using this method, most of the implanted FES systems utilizes 8 to 22 channels of stimulation to get good results (Johnston et al., 2003). The electrodes are generally implanted into the quadriceps, gluteus and lumbar erector spinae muscles bilaterally (Davis et al., 2001). Figure 1.3 shows such a system developed by Cleveland VA medical center and Case Western Reserve University (Agarwal et al., 2003; Forrest et al., 2011). It is called the VA/CWRU Standing System. The system has two main units: implanted unit and external unit. The implanted unit is composed of epimysial

and intramuscular electrodes, a wireless receiving and stimulating station, connecting wires, battery etc. The external unit is basically a control station for the implant, providing a clinical interface and control over the electrical stimulation. Clinical studies have demonstrated that using the implanted FES system motor complete SCI subjects have been able to stand for several minutes and take a few steps with the optional aid of ankle foot orthoses (AFO) (Guiraud et al., 2006). Some were even able to release one hand for a reaching task over their shoulder level while standing. Over 90% of body-weight was supported by most of the subjects reported (Quintero et al., 2010; del-Ama et al., 2012).

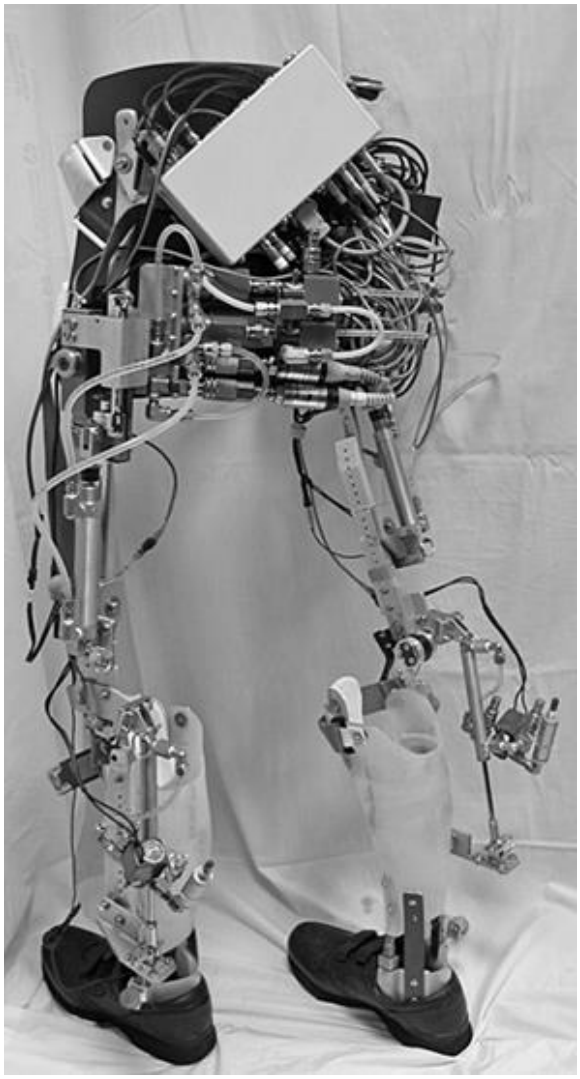

Figure 1.4 A hybrid system for walking (reprinted with permission from del-Ama et al., 2012)

Hybrid FES systems

Though some FES systems uses foot orthoses, hybrid FES systems generally use FES and Reciprocating Gait Orthoses (RGO) for foot, knee and back support to improve balance during standing and ambulation (Isakov et al., 1992; Greene and Granat, 2003). Another benefit of the hybrid FES system is reduced energy cost (del-Ama et al., 2012). RGO is essentially a knee-ankle-foot orthosis usually connected to a back brace by the hip joints and a cable coupling mechanism. Electrical stimulations are usually delivered to the rectus femoris muscle for hip flexion and to the hamstring muscles for hip extension (Kobetic et al., 2009).

Epidural spinal cord stimulation

Traditionally, epidural spinal cord stimulation (ESCS) is applied for pain relief (Kumar et al., 1998). But, some recent studies demonstrate its potential application in SCI rehabilitation (Hegarty, 2011). Different activity-based therapies such as Body Weight Supported Treadmill Training (BWSTT) has already been proven to be effective for restoring motor functions such as walking in patients with incomplete SCI (Wessels et al., 2010); however, motor complete SCI patients have not been significantly benefited by such interventions (Fouad and Pearson, 2004). In contrast, a recent study has demonstrated that a clinically motor complete paraplegic patient regained the ability of full weight bearing standing and assisted stepping by treadmill training combined with an epidural electrical stimulation in the lumbosacral region of the spinal cord (Harkema et al., 2011). This groundbreaking work was a result of knowledge gained from extensive animal studies to restore motor functions using similar methods after mid-thoracic (T7-T10) hemisection of the spinal cord (Ichiyama et al., 2005; Gerasimenko et al., 2007; Lavrov et al., 2008; Courtine et al.,

2009). Figure 1.5 shows a conceptual ESCS model (Carhart et al., 2004). An autonomous electrical stimulator (similar to a cardiac pacemaker) is implanted. The electrodes are epidurally placed near to T9 to L1 spinal segments.

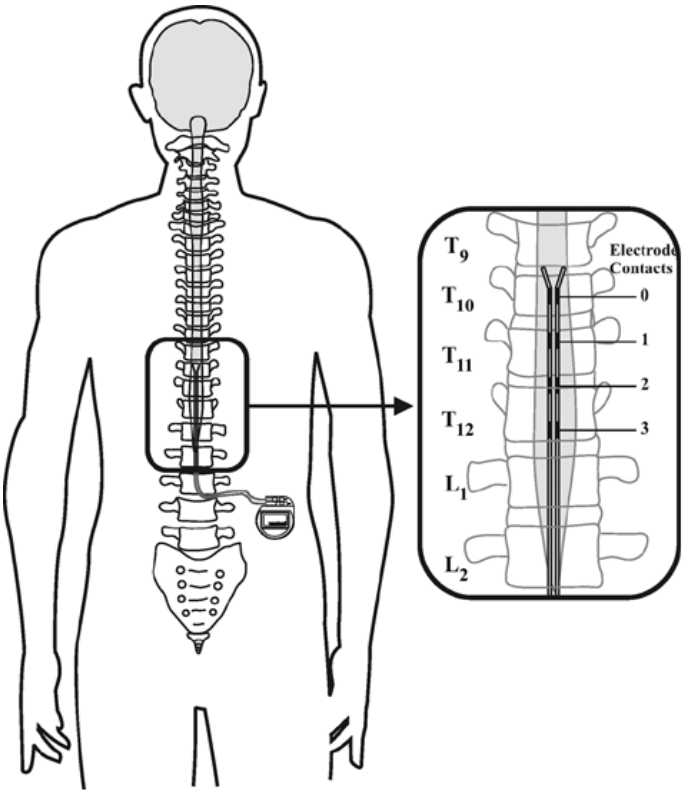

Figure 1.5 Conceptual diagram of epidural spinal cord stimulation. Electrode position is illustrated with a zoom view in the inset (reprinted with permission from Carhart et al., 2008)

While the exact mechanism behind this impressive recovery is still unclear, it is very difficult to predict the actual clinical impact of this new therapeutic method in a large SCI population. In rodents it was shown that following similar interventions, the injured spinal cord goes through massive changes of reorganization of their neural circuitry (van den Brand et al., 2012). In human patients whether this will happen or not is still unknown.

Motor complete SCI recovery with ESCS combined with activity dependent therapies have triggered the creation of a new concept of rehabilitation after SCI

(Edgerton and Roy, 2009). While it was a "proof of concept" that paralysis is unavoidable following complete SCI, these new results force a change in the traditional view of spinal cord and recovery therefrom; thus plasticity (Edgerton and Harkema, 2011). Moreover, clinically tested motor complete injuries may have some surviving tissue or neural connections passing the lesion site (Kakulas, 1984), providing hope of recovery using this new intervention (Edgerton and Roy, 2012). It is found that these neurons and their connections can actually control very complex movements when they receive appropriate sensory input with the aid of the excitability of this network by both electrical and pharmacological agents (He et al., 2006; Musienko et al., 2011). These experiments support the hypothesis that both spinal and supraspinal plasticity can induce recovery after SCI, and with proper sensory inputs this plasticity can restore significant functionalities like standing and walking (Edgerton and Harkema, 2011).

Intra-spinal microstimulation

Intra-spinal microstimulation (ISMS) is an *in vivo* stimulation technique placed in the vicinity of neural cell bodies in the spinal cord to artificially depolarize cell membrane potential by microampere current injection, resulting in activation of voltage gated channels and generation of action potentials. These action potentials propagate through the ventral horn of the spinal cord to the periphery and produce muscle contractions. ISMS has a number of advantages over muscle or peripheral nerve stimulation. Since all the lower-motor neurons that control lower-limb function are located in a small area of about 5 cm in the lumbro-sacral spinal cord region, by implanting multiple electrode array (MEA) in the lumbo-sacral region, one can access all the muscles related to locomotion (Mushahwar and Prochazka, 2004).

Moreover, by stimulating lower-motor neurons it produces more natural functional synergistic movements in contrast to muscle stimulation (Bamford and Mushahwar, 2011). A better selectivity, muscle force and recruitment order can be achieved by ISMS (Holinski et al., 2011). Muscle fatigue is also reduced during this stimulation.

ISMS has already been proposed for restoration of locomotion in SCI paraplegics (Mushahwar and Prochazka, 2004; Pikov, 2008). However, till now, most of the research being conducted has been on animal subjects. The results have been very promising, but there are certain barriers that still need to be overcome before applying in patients, which includes electrode-tissue biocompatibility electrochemically reversible charge injection capacity for electrode-tissue integrity, miniaturization of the implant, telemetry etc.

Motor mapping experiment on anesthetized cats demonstrated that ISMS in the ventral horn of the spinal cord generate selective and functional activation of hindlimb muscles (Mushahwar and Horch, 2000). Recent studies also revealed that the Rexed lamina VII, an intermediate region of the lumbosacral spinal cord, contains specialized neural circuitry for movement generation in the hindlimbs, as shown in Figure 1.6 (Mushahwar and Prochazka, 2004; Mushahwar et al., 2007). It is also suggested that rhythmic limb movement could be achieved by ISMS through a limited number of electrodes implanted in lamina VII (Pikov, 2008).

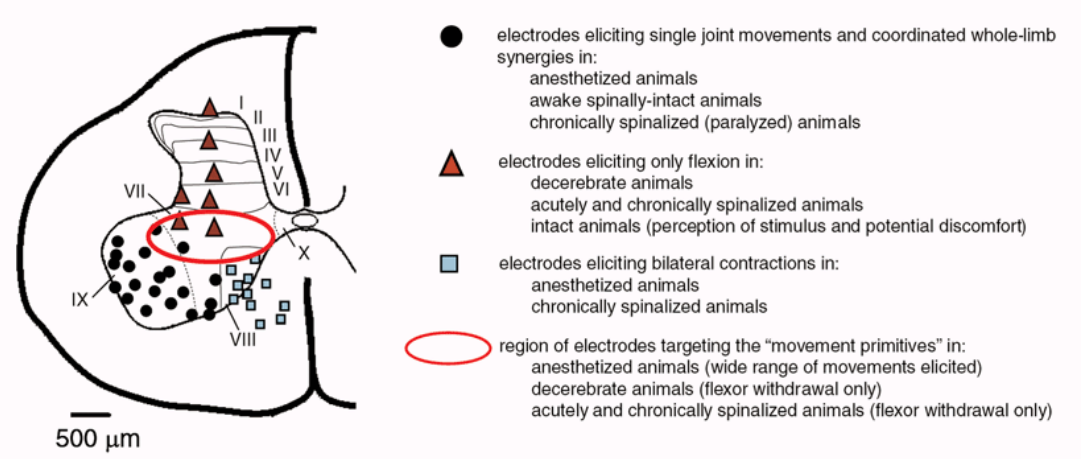

Figure 1.6 Lumbosacral spinal cord mapping of a cat (reprinted with permission from Mushahwar et. al, 2007).

One of the most significant findings has been that microstimulation in the intermediate regions of the grey matter predominantly evokes swing phase-like flexor reflex responses in signalized animals, whereas stimulation within the ventral horn generates strong extensor movements capable of body weight bearing during standing and stepping (Mushahwar and Saigal, 2002; Mushahwar and Prochazka, 2004). The generations of body weight bearing extensor synergies are of particular interest since they suggest that standing after SCI could be possible by using a few ISMS electrodes. Furthermore, ISMS in the ventral horn did not cause any apparent discomfort to the animals (Mushahwar and Horch, 2000). These findings are of great importance in developing spinal prosthetics for SCI patients that utilized ISMS.

We have witnessed that electrical stimulation of the muscles, nerves and even the neurons in the spinal cord provides functional recovery or augmented movements in SCI paraplegics. This stimulation along with proprioceptive inputs has enabled body weight bearing walking in both human and animal subjects (Carhart et al., 2004; Gerasimenko et al., 2007; Harkema et al., 2011). Though the exact mechanism and outcome is still unknown, it is expected that combining FES with locomotor training will potentially provide permanent spinal recovery by means of activity-

dependent plasticity for SCI patients. In addition, physical exercise and ESCS not only stimulate the production of endorphins and serotonins - two neurotransmitters, they also contribute to upregulating brain-delivered neuroptropic growth factors that may promote synaptic and functional plasticity within the brain and the spinal cord (Ying et al., 2005). It was also found that regular electrical stimulation of paralysed lower-limb muscles induced exercise related physiological changes that have some therapeutic benefits (Ragnarsson, 1988).

But all these stimulations (muscle, nerve or spinal cord) are manually controlled (operated by the user or therapist), therefore missing a natural "*intent*" driven mechanism. However, recent development in brain-machine interfacing research provides hope of developing direct cortical driven stimulation for these paralysed patients.

Brain-machine interfacing

Brain-machine Interface (BMI) is a neuroprosthetic approach for directly interfacing the brain with an artificial electronic system to record neural "*intent*" for a number of applications such as restoration of motor functions of paralysed people (Nicolelis, 2003; Lebedev and Nicolelis, 2006; Jackson and Zimmermann, 2012), and the operation of robotic devices (Collinger et al., 2012; Hochberg et al., 2012; Wang et al., 2013) or a computer (Hochberg et al., 2006). In BMI for neuroprosthetics, generally the motor cortex is interfaced with multiple electrodes to record movement related neural information. This recording can be invasive (single or multi-unit spikes), semi-invasive (ECoG - electrocorticogram) or noninvasive (EEG - electroenciphalogram). Invasive BMI has attracted more attention as it allows higher spatiotemporal resolution of information for decoding, and thus better functionality

for prosthetic control (Lebedev and Nicolelis, 2006). In invasive motor BMI, usually a Multiple Electrode Array (MEA) is implanted into the subject's primary motor cortex to record neuronal spikes (Kralik et al., 2001; Lebedev et al., 2008; Turner et al., 2008). Then, a neuroprocessor performs the online classification of these spikes and decodes the neural "*intent*" of movements (Linderman et al., 2008; Zacksenhouse and Nemets, 2008; Churchland et al., 2012) to generate adequate control signals for prosthetic limbs (Chapin et al., 1999; Collinger et al., 2012; Hochberg et al., 2012; Wang et al., 2013) or even stimulates paralysed muscles (Moritz et al., 2008; Ethier et al., 2012) or the spinal cord (Nishimura et al., 2013) for movement generation. Figure 1.7 shows a typical BMI setup for prosthetic control (Leuthardt et al., 2006).

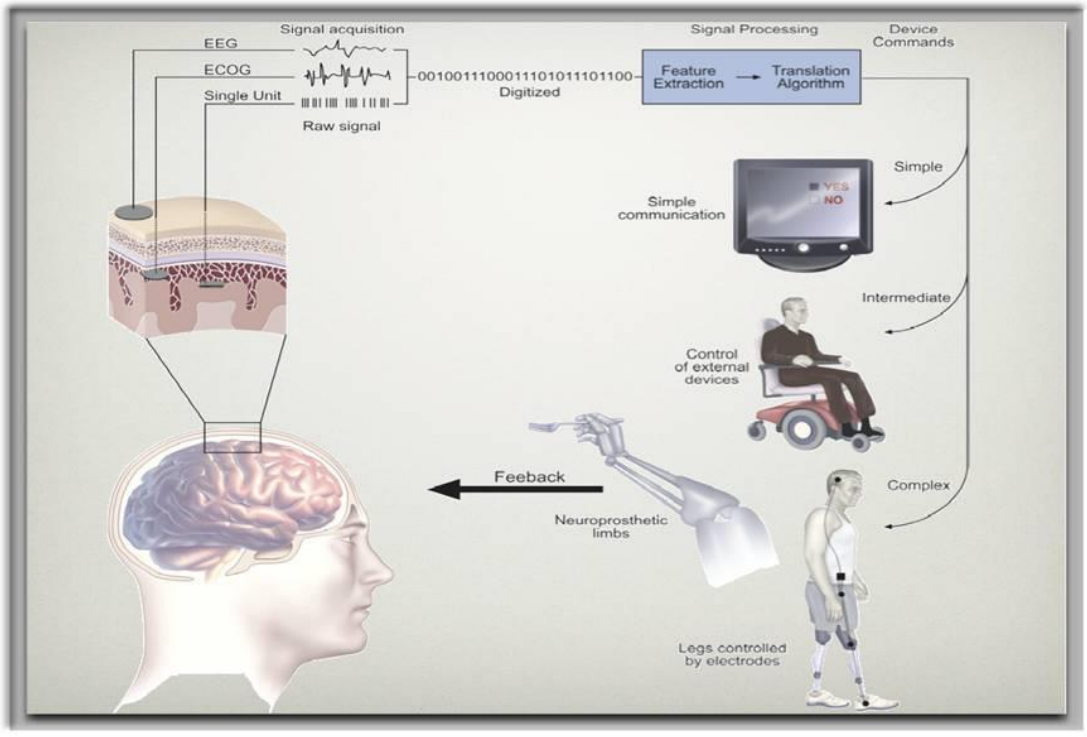

Figure 1.7 Generalized brain-machine interface (BMI) system (reprinted with permission from Leuthardt et al., 2006)

Generally, cortical activities are recorded by an electrophysiological data acquisition system in one of the forms of EEG, ECoG or single or multi-unit

extracellular spikes. These neural ensembles of recording are then processed by a neural signal processor encompassing with feature extraction and translation algorithms for the online prediction of intention of movement and generate control commands for the prosthetic device such as a computer, wheelchair or a prosthetic limb (as illustrated in Figure 1.7). Importantly, in BMI, the movements of any of these artificial systems must provide some sensory feedback to the subject. Usually this is done by natural visual feedback. A better user concentration is needed as there is no other feedback with current BMI systems (Cipriani et al., 2008; Eskandari and Erfanian, 2008).

In recent years, BMI has undergone significant progress in the development of upper-limb neuroprostheses (Lebedev and Nicolelis, 2006; Fifer et al., 2011; Lebedev et al., 2011). Recent studies demonstrated quadriplegics operating a computer cursor (Hochberg et al., 2006) and a robotic arm (Collinger et al., 2012; Wang et al., 2013) using this technology. In non human primates it has been demonstrated that a paralysed limb can be operated through this BMI system (Moritz et al., 2008; Ethier et al., 2012). However, all these BMI setups require the subject to be physically attached to a connector composed of a bundle of electrical wires through a head socket. Figure 1.8 shows the first successful BMI system, called BrainGate™ (Hochberg et al., 2006) that utilizes such method. It might be suitable for the experimental phase, but for clinical application wireless implant is inevitable (Kim et al., 2009; Zhang et al., 2012; Dethier et al., 2013).

Figure 1.8 BrainGate™, a tethered BMI system developed by Donoghue and colleagues (reprinted with permission from Hochberg et al., 2006)

Development of a reliable neural interface between the neural tissue and the external electronics is one of the major challenges for successful neuroprosthetics (Cogan, 2008). This interface should be bi-directional by means of both recording from the neural tissue and providing sensory feedback (Rouse et al., 2011). Our nervous system is closed loop by nature as we continuously receive sensory inputs about our posture and motor actions (Kandel et al., 2000). This continuous sensory-motor interaction is important for learning skilled motor tasks and is essential for adaptive movements (Yu et al., 2009; Chan et al., 2011). Otherwise the control would not be precise and manageable (Lundy-Ekman, 2002). For future neuroprosthetic devices the system should also be closed-loop to give sensory feedback on the motor actions. This could be done by stimulating the somatosensory cortex with external current, called intracortical microstimulation (ICMS) as shown in recent studies (O'Doherty et al., 2009; Medina et al., 2012; O'Doherty et al., 2012).

Physiological basis of locomotion

Although locomotion such as walking seems to be a simple repetitive motor activity, the neural mechanisms behind this are rather complicated and extensive. A simple walking requires spatiotemporal coordination of limb joints and the neuromuscular systems, their adaptations and controls. It has been a major topic of research for the last many years ranging from mammalian to primate animal models. For many species the rhythmic electrical activities are generated by sets of neural networks (Dietz, 2003). This is generally referred as Central Pattern Generator (CPG), located in the spinal cord in most of the animals. In combination with afferent sensory inputs, these pattern generators (CPGs) work with the motor periphery to generate repetitive motor acts during locomotion. Figure 1.9 shows a general model of CPG (Van de Crommert et al., 1998). Figure shows that the CPG contains extensor and flexor half-centres (EHC and FHC, respectively) that have inhibiting inputs to each other. Hence, during end of each phase (stance or swing) EHC and FHC works are reciprocals. During the stance phase, load of the lower limb is detected by group I extensor afferents and group II cutaneous afferents which activate the EHC. Due to the positive feedback loop through EHC, the extensor activity is reinforced during the loading period of the stance phase. At the end of the stance phase, group Ia afferents of flexor muscles excite the FHC and thereby initiate the onset of swing phase. Since, there is no extensor load during the swing phase; the EHC does not inhibit the FHC which facilitates the swing phase to complete the cycle.

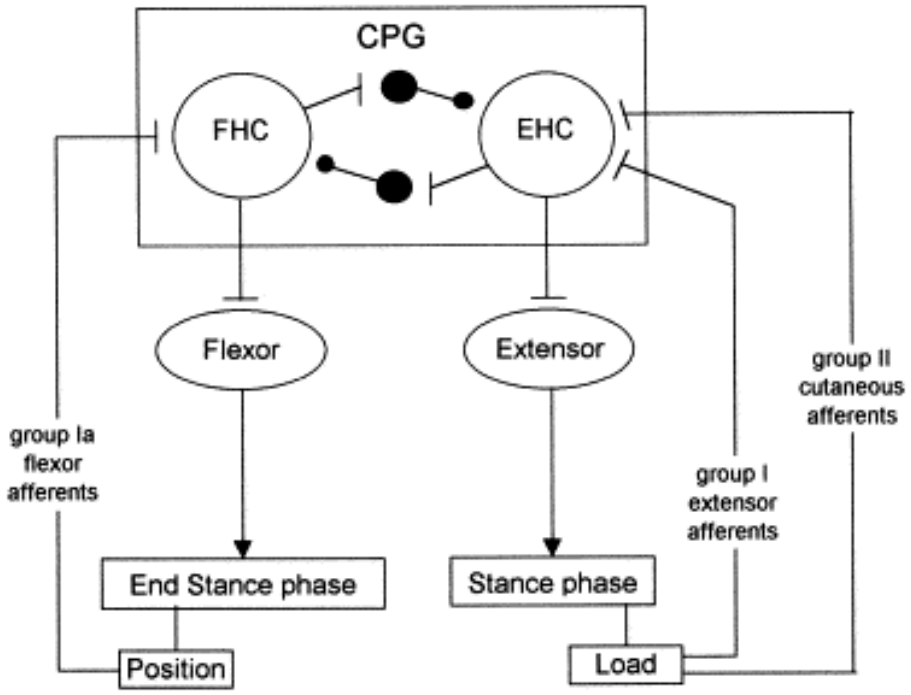

Figure 1.9: Central Pattern Generator (CPG) model diagram (reprinted with permission from Van de Crommert et al., 1998). The core of a CPG is a mutually inhibitory extensor half-center (EHC) and a flexor half-centre (FHC).

It is assumed that for cat, there is at least one such CPG for each limb that are located in the spinal cord. A decelerated cat demonstrated full-weight bearing walking on a moving treadmill belt (Miller et al., 1975), suggesting such existence of pattern generators. However, for primates there is still a controversy of the existence of similar CPGs (MacKay-Lyons, 2002). Although, extensive locomotor training after SCI showed partial or even full regain of walking function which strongly supports the view that there exists a human CPG for locomotion (Duysens and Van de Crommert, 1998). However, it is possible that the primate gait relies less on spinal automatisms and more on supraspinal controls for the expression of the locomotor activities.

Rationale of the current study

While BMI has demonstrated the feasibility of upper-limb neuroprostheses, it has not yet been evaluated for the restoration of the lower-limb motor functions of disabled. Not enough BMI studies have been conducted on the development of lower-limb neuroprosthesis, except a few (Pfurtscheller et al., 2006; He et al., 2008; Weiguo et al., 2009; Manohar et al., 2012). Though some studies show that locomotive information can be captured from cortical recordings (Fitzsimmons et al., 2009; Alam and He, 2013), no significant work has been done to restore lower-limb function in paralysed patients using this technology (Lebedev et al., 2011). All BMI research largely neglects restoring locomotion functions in SCI paraplegics.

Most of the BMI systems utilize hundreds of neural cells for recording and complex computer algorithms to decode the cortical "*intent*" for movements (Wahnoun et al., 2006; Zacksenhouse and Nemets, 2008; Churchland et al., 2012). However, there is still a debate over whether many neurons population decoding with advanced computer algorithms is better than a small number of neural recordings with their direct control or not (Scott, 2008). A recent study showed that a monkey could voluntarily control a computer cursor by continuously modulating the firing of a single cortical neuron (Moritz and Fetz, 2011). But, it is still unknown whether small neural population recordings can provide step gait cycle information or not; and whether this lower-limb BMI can be utilized for restoring locomotion in paralysed also needs to be explored. In this research study all these questions have been addressed.

Conceptual and experimental model

Figure 1.10 illustrates the conceptual model of lower-limb BMI in SCI paraplegics. It is essentially an electronic spinal bridge, named "Motolink" capable of bypassing cortical signal across the lesion of spinal cord.

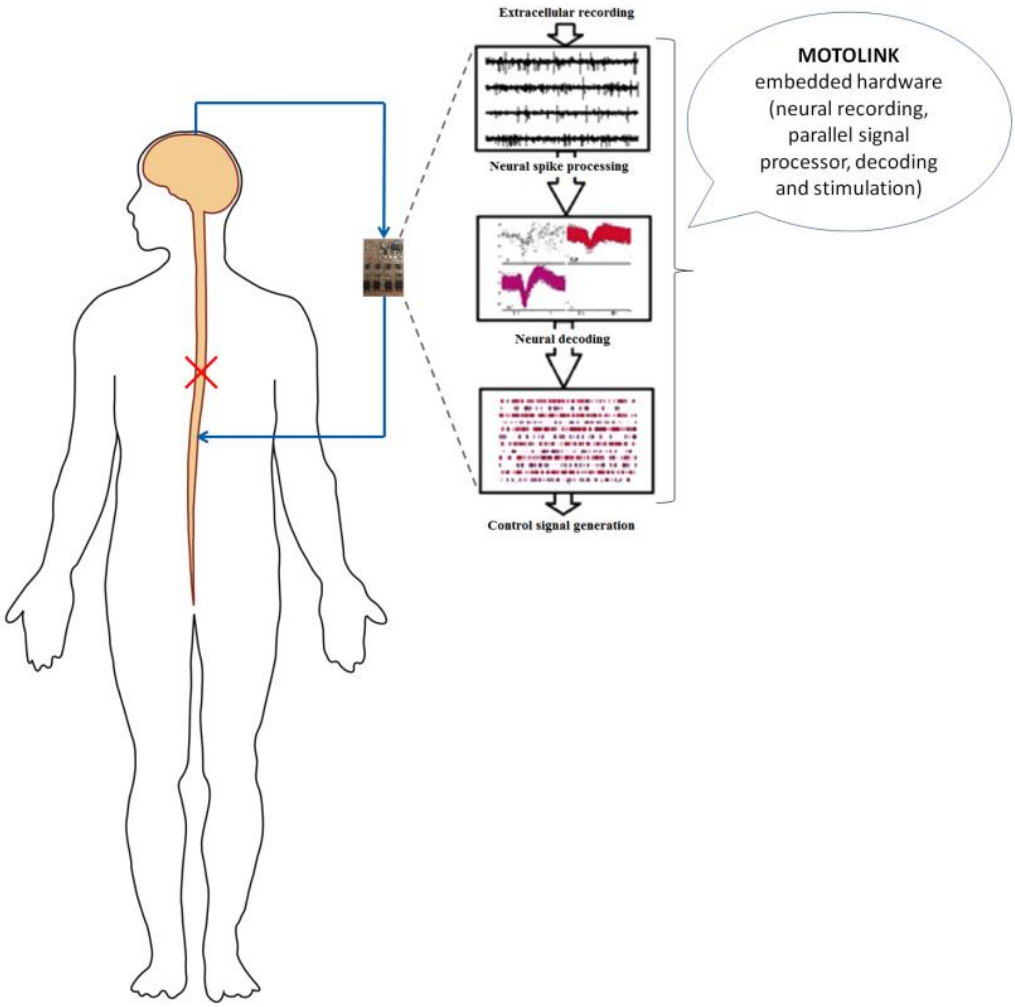

Figure 1.10 Conceptual diagram of a brain-machine-spinal cord neuroprosthetic system.

To establish the above illustrated solution for SCI paraplegics experimental models being utilized. Non human primates and rodents are well established animal models for BMI research. Hence, spinal rats were utilized in the current study.

Research questions

In this research study I addressed the following questions:

1) Whether different step gait-related neural information can be captured in parallel from rats' primary motor cortex during walking? and

2) Whether and how this neural information can be utilized to restore locomotion after complete spinal transection?

Research hypothesis

It is hypothesized that there is cortical "*intent*" linked to hindlimb movements during forelimb walking in rats; reflected by neural signals.

Study design and objectives

In the current study, spinal rats were used as the animal model to design and develop lower-limb BMI for locomotion. The hindlimb area in the primary motor cortex of rats was utilized to record the neural "*intent*" of locomotive information during treadmill walking before and after spinal transection (mid-thoracic). Finally, a novel BMI device was developed to process this real-time neural information for electrically activating paralysed hindlimb muscles to mimic forelimb stepping on a treadmill.

Outline of the thesis

The thesis is composed of six chapters. Present one is the introduction of the project stating background of current problem, proposed solution, scientific questions, hypothesis and experimental designs of the research.

Chapter two describes the experiments conducted in healthy rats to extract locomotive information during treadmill walking.

Chapter three describes the experiments conducted in spinal rats to compare extracted locomotive information before and after mid-thoracic spinal transection during forelimb walking.

Chapter four is the design and development of artificial spinal bridge hardware called “Motolink”.

Chapter five is the experimental test of the “Motolink” hardware in spinal rats to stimulate the hindlimb for cortical neural signals to restore movement.

Chapter six is the conclusion of current research study and suggestion for future research.

CHAPTER 2: EXTRACTING NEURAL INFORMATION ON LOCOMOTION FROM CORTICAL RECORDINGS

Background

While neuroprostheses have been successfully evaluated for the restoration of upper-limb functions, very little research has been accomplished of developing such systems for restoring lower-limb motor functions, except for a few studies (He et al., 2008; Fitzsimmons et al., 2009; Weiguo et al., 2009; Manohar et al., 2012; Alam and He, 2013). Among them, two studies on non-human primates demonstrated cortical signals that are potentially available for hindlimb neuroprostheses.

In the first study, He and colleagues reported successful recording of cortical signals for standing and squatting with aid of a customized sitting apparatus for monkeys (He et al., 2008). With fixed head position, the monkey can push down a movable pedal to emulate standing and flex the legs to release the resistance that counterweights to emulate squatting down. A microwire array was surgically implanted into the hindlimb area of primary motor cortex (M1). Neural recordings were accomplished during the sit-stand-sit task. In this task, the subject was trained to play a customized computer game to get food rewards. Total 1633 neural units were recorded from the hindlimb area of motor cortex. Among them, about one-quarter units (323 neurons) significantly increased their firing rates during sit-to-stand transition (with the initiation of the leg extension to push up the body); and almost half of the units (784 neurons) were closely correlated with either the actual action of extension or flexion or holding the hindlimb position against a weighted pedal. The remaining neural units did not show any significant correlation with the task. The result suggests that these neural signals are potentially available to be utilized in lower-limb neuroprostheses.

In the second primate study, detail locomotive information was decoded from the cortical recordings. Microwire arrays were implanted in the primary motor (M1) and primary somatosensory (S1) cortices of two female macaque monkeys for neural recording in a locomotion experiment (Fitzsimmons et al., 2009). The subjects were trained to walk bipedally on a customized treadmill with a supporting hand bar, placed within reach of the monkey's arms to allow balance and stability during walking. Each of the monkey's leg and arms were unrestrained during the experimental walking sessions. After about one month of training the monkeys had learnt to walk bipedally on the treadmill. Fluorescent markers were placed on monkey's right leg and high speed video was captured to extract different kinematic information. During the experimental session, a total of 180 to 238 well sorted single unit neural spikes were recorded in monkey 1, and from 173 to 334 units in monkey 2. Statistical analysis (Wilcoxon signed rank test) confirmed that the average neuronal firing rates increased during walking in both M1 ($p < 0.001$) and S1 ($p < 0.001$) in each monkey. From this neural ensemble recording, kinematic variables such as gait positions, hip and knee angles, step time, step length, foot location, foot orientation etc. were successfully predicted using a series of independent linear decoders (multiple Wiener filters). It was also found that recording of a larger neuronal population was needed for accurate prediction of walking patterns during more complex walking talks. However, extraction was further improved using a switching decoder that designated as a sub-model of each walking paradigm. A remote humanoid robot was demonstrated to walk in real-time half way across the world using this cortical recording and decoding algorithm (Lebedev et al., 2011). The monkey received real-time visual feedback of the robot's walking on a video screen during the task.

In a rodent study, it has been shown that multiple types of movement-related information encoded in hindlimb/trunk cortex that is potentially available for neuroprosthetic controls. In that study, rats were mounted with a pelvic orthosis to apply forces directly to the skeleton (Weiguo et al., 2009). Tetrodes array was implanted in the hindlimb/trunk area of rats' primary motor cortex (M1). During treadmill locomotion, multiple hindlimb/trunk related kinematic variables under normal and loaded condition were successfully decoded using linear regression during treadmill locomotion. The result showed that the decoding of robot/pelvis position and hindlimb posture (joint angles and positions) were better than the decoding of kinematic velocities for both robot/pelvis attachment and the hindlimb (paired *t*-test, $p < 0.05$). It was also found that the proximal variables were better represented than the distal variables, whereas, pelvic motion was better reconstructed than any other motion features (paired *t*-test, $p < 0.05$). These data suggest that hindlimb/trunk cortical area in rat best encodes proximal and task level variables useful for position coding, while leaving the detailed execution of locomotion to other level (most likely in low spinal level) in this task set.

The above three studies show the importance and potential of cortical signals both in primate and rodent useful to generate the control signals for hindlimb neuroprostheses. To address additional important question: whether step gait related information can be captured in parallel from rats' cortex, in the current research study, experiments were designed to record and analyze cortical signals from rats motor cortex during treadmill walking. The detail experimental methods are described in following section.

Methods

All experiments were conducted in compliance with the guide for the care and use of laboratory animals (National Institutes of Health, Publication No. 86-23, revised 1985). The Animal Subjects Ethics Sub-Committee of the Hong Kong Polytechnic University and the animal regulatory body of the Department of Health in Hong Kong approved all experimental procedures. The experimenter held a personal license for animal surgery.

Experimental Subjects

Twelve healthy female Sprague Dawley rats weighing 250–350 g served as subjects in this study. The rats were housed in the Centralized Animal Facilities at the Hong Kong Polytechnic University at a constant temperature of 22°C and on a regular 12 h light/dark cycle. Diet was carefully maintained to keep body weight within a suitable range.

Animal training

Over the first few days of the study the rats were introduced to a custom-modified treadmill that had three chambers of different widths for walking, separated by acrylic plastic, shown in Figure 2.1. The rats practiced walking on the moving treadmill belt at different speeds (4–6 m/min) for 1 min. The walking sessions were separated into less than 1 min break for rest. Generally, 10 to 30 walking sessions were accomplished by each rat for a day. Food and water rewards were delivered at the front of the treadmill to keep the rat interested and facing forward. To speed up the learning process, two rats were placed into two different chambers at the same time: one that had already mastered the walking task and one that was new to the

task. The treadmill was remotely controlled from outside of the experiment room. A video camera (Pleomax™, Samsung C&T Corporation, Korea) was utilised to monitor and record the walking task.

Figure 2.1 Experimental setup for treadmill walking task.

Microwire array for neural recording and stimulation

We developed custom microwire arrays for recording and stimulation (Figure 2.2). Each microwire array was composed of seven recording electrodes, one stimulation electrode, one reference electrode, and one common terminal wire. Recording and reference electrodes were Teflon-coated tungsten microwires (A-M Systems, USA), and the stimulation electrode was stainless steel. Nine polymethyl methacrylate tubes (Polymicro Technologies, USA) were glued-fixed with 500 μm spacing onto a paper base, and a microwire array (length, 6 cm) was inserted and glued into each polymethyl methacrylate tube. The reference electrode was kept about 500 μm longer than the recording and stimulating electrodes, and 200–300 μm at the tip of

the reference electrode was exposed. Conductive metal wire was utilised as the common terminal of the array electrodes. All microwires from the array and the common wire were soldered to a 20-pin female connector (two rows, 1.27 mm pitch) and insulated with silicon glue (Tec-bond 240, Power Adhesives Ltd., Essex, UK).

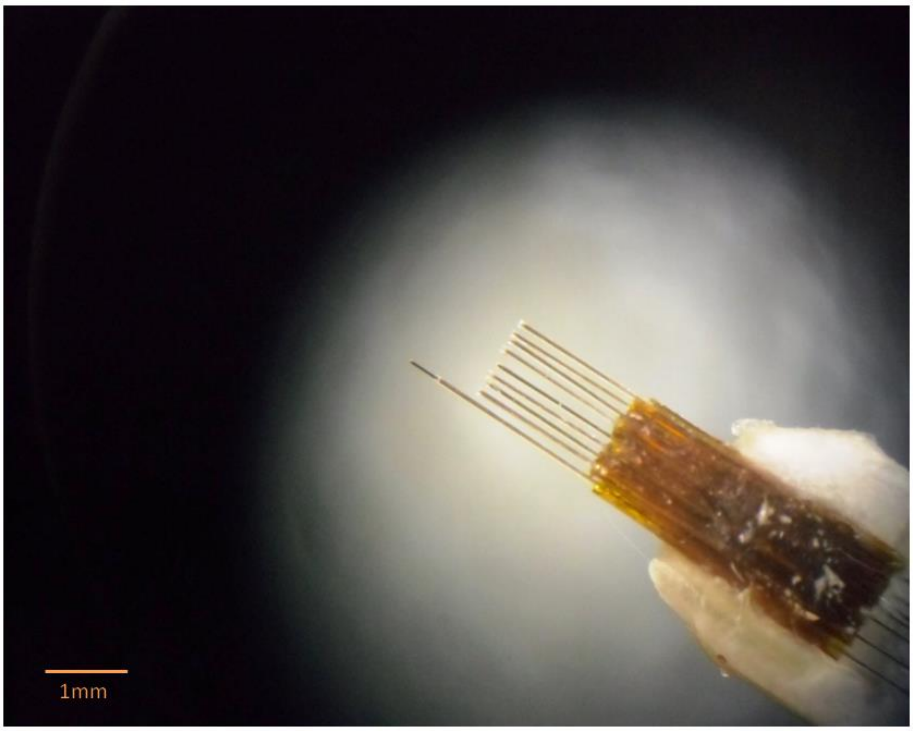

Figure 2.2 Custom made microwire array. The reference electrode is longer and more exposed than the recording and stimulating electrodes (shown by left most electrodes in the array).

Cortical implantation

All surgeries were performed in aseptic conditions. Animals were pretreated subcutaneously with atropine sulphate (0.05 mg/kg, Sigma, USA) to restrain tracheal secretions. About 10 min after atropine injection, anaesthesia was induced intraperitoneally with 50 mg/kg pentobarbital sodium (54.7 mg/ml solution, Ceva Sante Animale Co., France) and maintained by supplemental doses (10 mg/kg/h, i.p.). The subject was mounted in a stereotaxic device and body temperature was

controlled and maintained between 37 and 38°C by a homoeothermic system (Harvard Apparatus, USA). After a midline incision was made in the scalp, a small craniotomy (approximately 3 mm × 2 mm) was performed across the bregma line, shown in Figure 2.3.

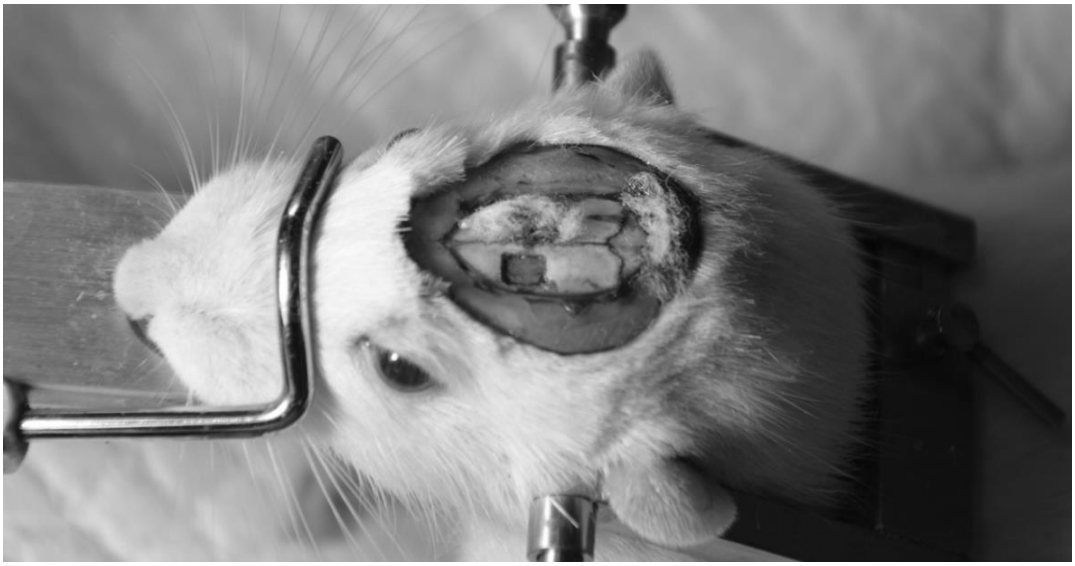

Figure 2.3 Craniotomy of an anesthetized rat with exposed left motor cortex.

After carefully removing the dura, the microwire array was slowly inserted (100 μm/min) into the hindlimb area of the left M1 using a stepping-motor micro-manipulator (Narishige, Japan) that was controlled remotely from outside the surgery room. The array was placed according to previous reports (Neafsey et al., 1986; Fonoff et al., 2009), and placement is shown by the dotted area in Figure 2.4. Six metal screws were inserted into the skull, and the ground wire was wrapped around one of the screws. Neural recording and stimulation was conducted through the 20-pin socket to which the microwire array was connected. Continuous recording during the insertion of the array was accomplished using an amplifier (A-M system differential AC Amplifier Model 1700, Sequim, USA) with band-pass filter (0.3–5.0 KHz). The position of the array in the hindlimb area was confirmed by electrical stimulation and visual observation of the movements of right hindlimb.

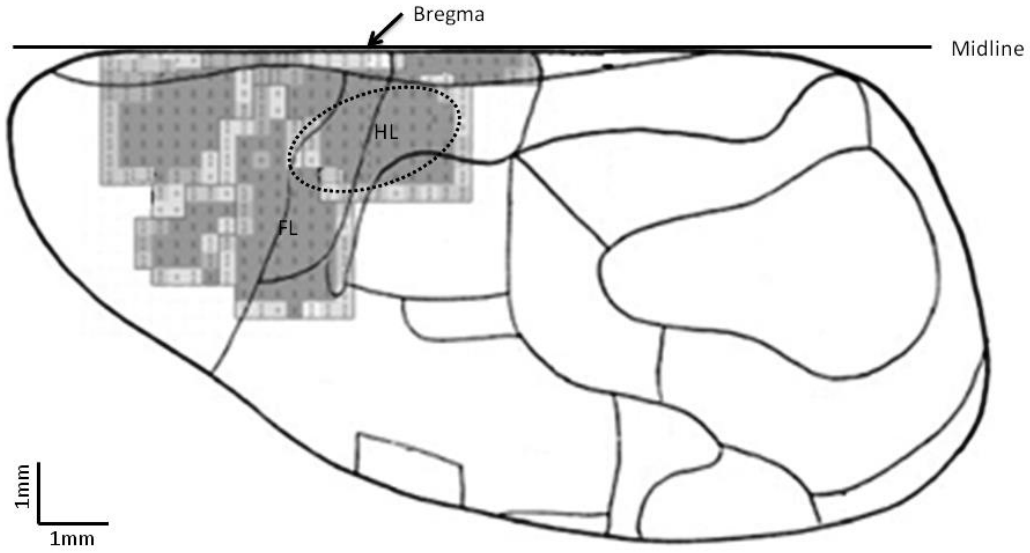

Figure 2.4 Electrode placements with reference motor map (Fonoff et al., 2009). HL: Hindlimb. FL: Forelimb.

The opening of the skull was covered with a thin layer of silicon epoxy (World Precision Instruments Inc., USA), and a layer of dental cement (Durelon™ Carboxylate Cement, Germany) was used to cover the microwire array, screws, cables, lower portion of the socket, and exposed skull.

Neural signal recording during treadmill locomotion

After 2–3 days of recovering from the surgery, rats were placed onto the treadmill for adaptation. Each rat performed 5–10 practice trials of 1 min length at constant speed (optimum treadmill speed was set according to each subject walking speed). Neural signals were recorded using an amplifier (A-M system differential AC Amplifier Model 1700, Sequim, USA) connected to the head connection, and a miniature (1 cm × 1 cm × 0.4 cm) three-dimensional accelerometer (ADXL335, Analog Devices Inc., USA) was attached to one hindlimb (see supplementary video 1). The accelerometer was used to identify the step cycles during gait. 10–20 recording sessions each of 1 min length were performed. During all recording sessions continuous video records

were made for further analysis using a video camera (Pleomax™, Samsung C&T Corporation, Korea). Data were digitised at 25 KHz using Axon Digidata 1440 (Molecular Devices Co., USA) and visualised in real time (Axon scope 10.0, Molecular Devices Co., USA) during each experimental session.

Data analysis

The data were analysed offline using custom-scripts written in MATLAB (MathWorks, Nitick, USA). Extracellular data were processed utilising Axon Clampfit 10.0 (Molecular Devices Co., Chicago, USA). Neural spikes were detected and sorted using a MATLAB-based open source electrophysiological data processing toolbox (Xiao-qin et al., 2011). Neural spikes rate were compared with the reference time signals from the accelerometer to determine the relation between step gait cycles and neural spikes.

Neural activity was studied during the transition from stand-to walk and from walk-to-stand. Neurons active in the stand-to-walk transition were named *Start* units, and neurons active in the walk-to-stand transition were named *Stop* units. For each unit, spikes were first binned into 50 ms and then a Perievent Time Histogram (PETH) was built by using the transition point from stand-to-walk as time 0. Activities from 1.5 s to 1s before the transition time were used as baseline. For each 50 ms bin in this PETH, normalized firing rate values were calculated by substracting the mean firing rate of the baseline and then by dividing by the standard deviation of the baseline. Finally, normalised firing rates of all *Start* and *Stop* units were generated, and units were grouped according to their firing rate patterns.

Raster plot and spikes time histogram were generated for each detected unit. For step gait cycles each step time was first converted into percentage. A full cycle

represents from 0 to 100%; where 30% is stance phase and the rest 70% is swing phase. Then spikes were binned into each 5% (18°) and then a Phase Histogram (PH) was built for each unit. Raster plots and spikes time histograms were also generated for each detected unit.

Data analysis and graphing software, Origin (OriginLab Corporation), SPSS (IBM Corporation) and MATLAB were utilized along with Microsoft Office tools.

Results

Locomotive information captured from rat's motor cortex during treadmill walking

For each subject, about 10 to 20 single units were identified and sorted from the cortical recordings during treadmill locomotion task. Figure 2.5 shows the average firing rate per cortical unit. The top panel illustrates the time raster of each single unit, while the bottom panel is the total spike counts per 50 ms time bin. Walking started at 2.2 sec while the treadmill started to move at 1.3 sec during standing and the treadmill stopped at 8.1 sec (shown by dotted lines). The walking also stopped at 8.1 sec (shown by the gray area).The total recording was done for 10 sec. The firing rate (Hz) was generally high during the walking time. However, the highest firing rate (~ 60 Hz) occurred just before (~ 200 ms) starting of walking. During the course of walking there are rhythmic increases of firing rate that likely indicates step gait cycles.

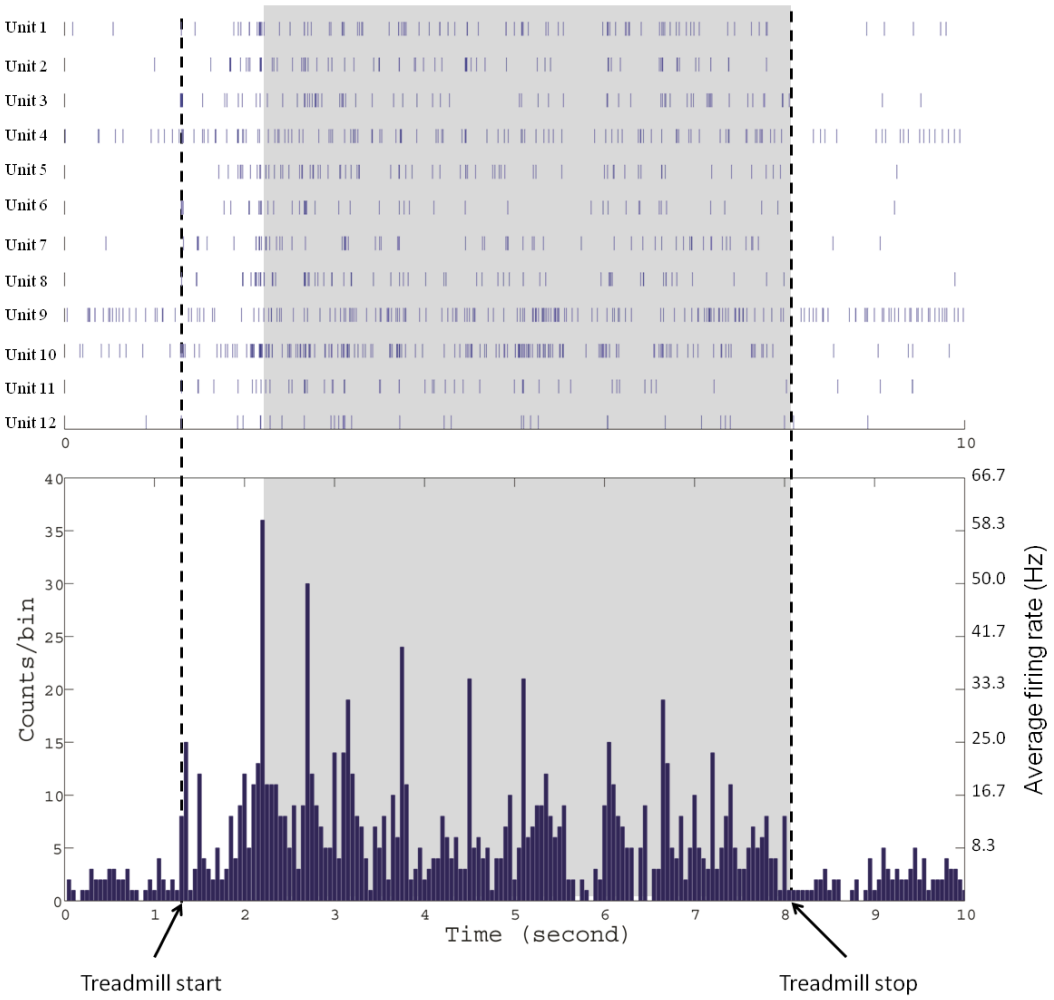

Figure 2.5 Average firing rate of cortical single unit during treadmill locomotion task. Gray area indicates the time of walking, while the rest white areas are standing. The dotted lines indicate the treadmill start and stop time.

Neuronal responses during stand-to-walk and walk-to-stand transition

The neural spike activities during the transition from stand-to-walk and walk-to-stand were studied. For stand-to-walk transition the units are named as *Start* units, while, walk-to-stand units are named as *Stop* units. Firing rates patterns of all *Start* and *Stop* units were analyzed. After normalization total four groups of *Start* units (according to the firing rate patterns) were identified, as shown in Figure 2.6.

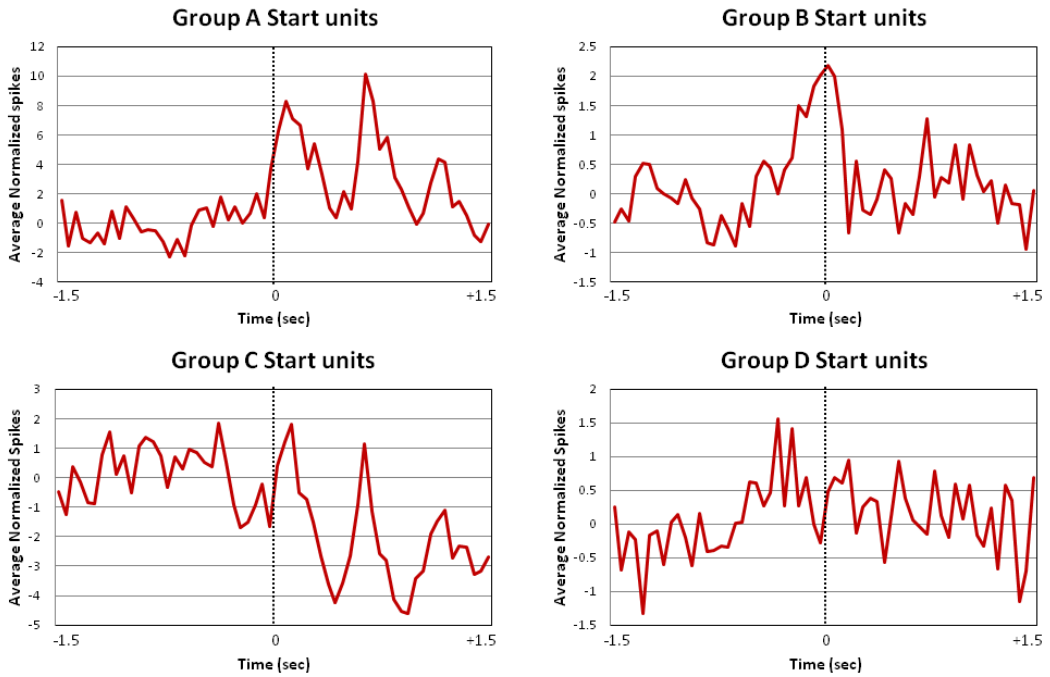

Figure 2.6 Average normalized spikes rate during stand-to-walk transition for four groups of neural units. The dotted lines indicate walking activation time.

Total 80 single units were analised from all the subjects.

Group A *Start* units: 25% single units are grouped into this category. Their firing rate patterns exhibited three positive peaks from the onset of walking.

Group B *Start* units: 32.5% single units are grouped into this category. Their firing rate patterns exhibited a single positive pick at the onset of walking.

Group C *Start* units: 10% single units are grouped into this category. Their firing rate patterns exhibited three positive peaks but with decreasing baseline firing rates from the onset of walking.

Group D *Start* units: 32.5% single units are grouped into this category. No distinguishable firing rate pattern could be identified for this category of neurons during this task.

Similarly, walk-to-stand transition, that is, *Stop* units were identified and grouped into four categories, as shown in Figure 2.7.

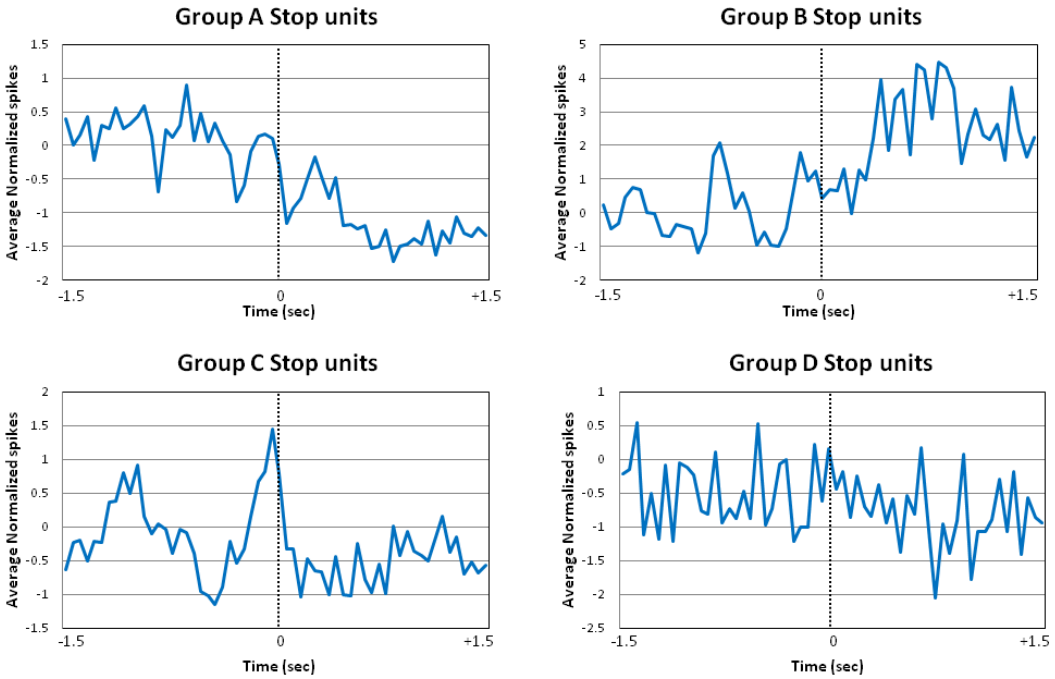

Figure 2.7 Average normalized spikes rates during walk-to-stand transition for four groups of neural units. The dotted lines indicate the standing from walking.

Similarly, total 80 single units were analised from all the subjects.

Group A *Stop* units: 37.5% single units are grouped into this category. Their firing rate patterns exhibited decreasing baseline firing rates from the onset of standing.

Group B *Stop* units: 10% single units are grouped into this category. Their firing rate patterns exhibited increasing baseline firing rates from the onset of standing.

Group C *Stop* units: 20% single units are grouped into this category. Their firing rate patterns exhibited a positive pick at the onset of standing.

Group D *Stop* units: 32.5% single units are grouped into this category. No distinguishable firing rate pattern could be identified for this catagory of neurons during this task.

Neuronal responses during steps gait cycles

A moderate speed for the moving treadmill belt was found and set for comfortable walking for the subjects. The mean step time was recorded 0.73 sec (standard deviation of 0.118 sec) in healthy subjects, as sown in Figure 2.8. Fitted normal distribution curve is shown in the figure.

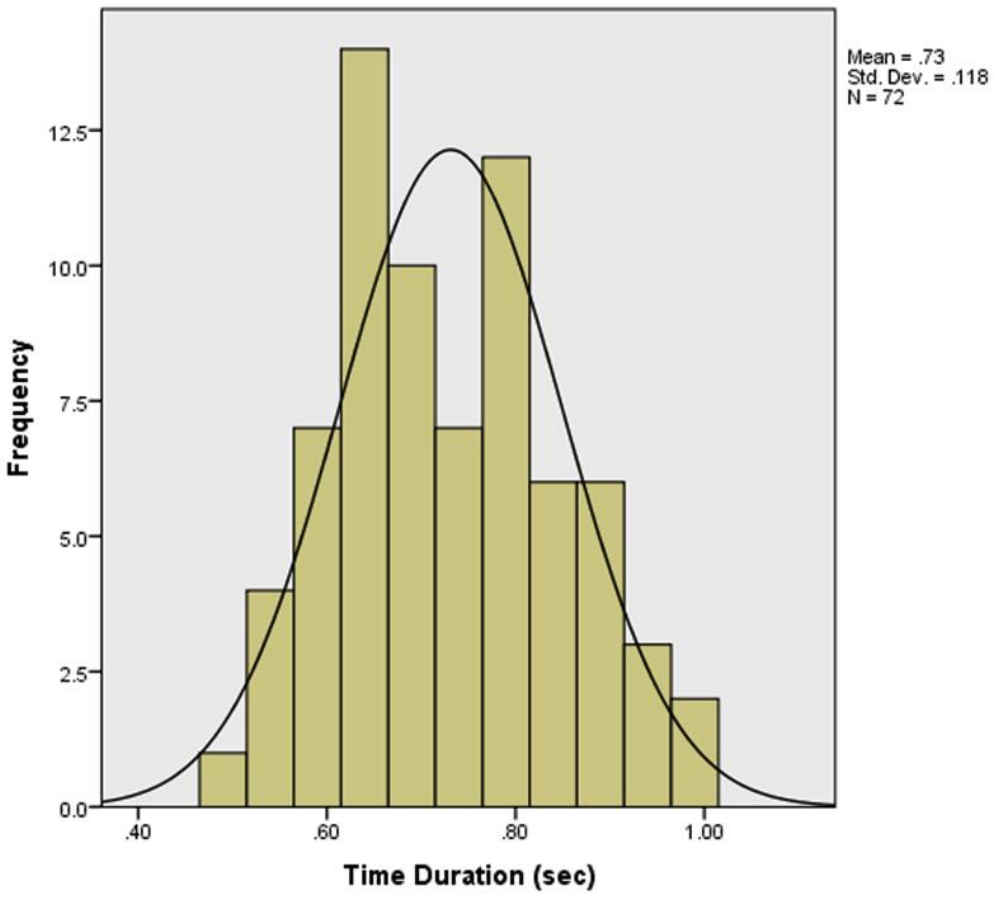

Figure 2.8 Step time histogram with a fitted distribution curve of walking indicates average one step time of 0.73 sec (SD: 0.118 sec) in healthy subjects.

During walking some neural units demonstrated rhythmic firings of their spikes. In each steps they are tend to fire in predominant gate phase, as shown in Figure 2.9. These neurons are considered of having best rhythmic patterns (R-square value > 0.65) during walking steps. The gray area of each cycle is stance phase while the rest is swing phase of one step.

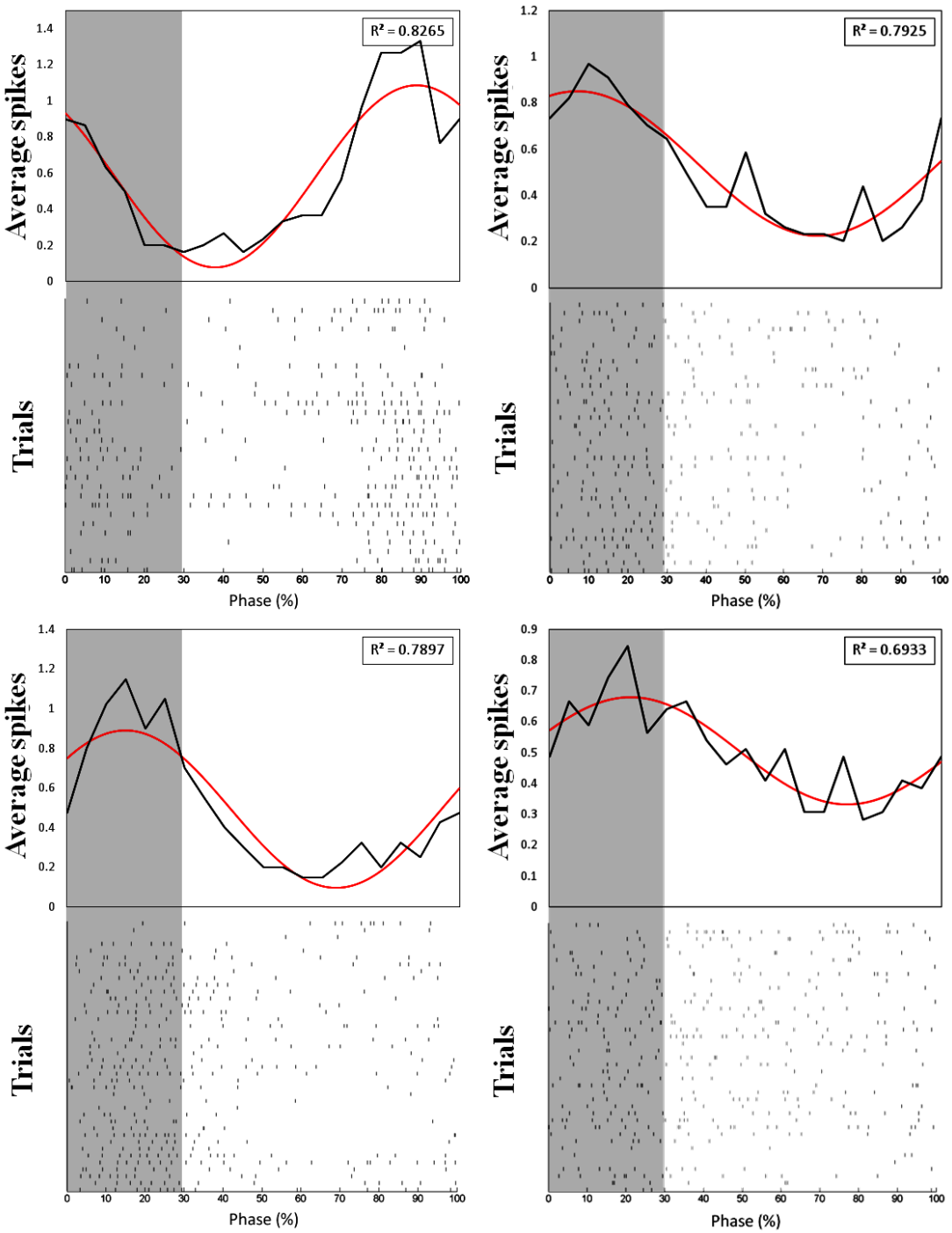

Figure 2.9 Average spikes per bin of four selected best units. Each panel represents one neural unit. The upper panel shows the average firing rate (black line) expressed relative to the step gait cycle in intact rats, and the lower panel shows the raster plot. A sinusoidal fitting line is shown in red and the adjusted R-square value for this fitting is presented in each panel. The grey area is swing phase and the rest is the stance phase of one gait cycle represented in percentage.

Some neurons with lower significance of modulation during walking were also analyzed. During walking they also tend to fire in predominant gate phase but with lower significance (Figure 2.10). These neurons are considered of having moderate rhythmic patterns (R-square value < 0.65) during walking steps. Similarly, the gray area of each cycle is stance phase while the rest is swing phase of one step.

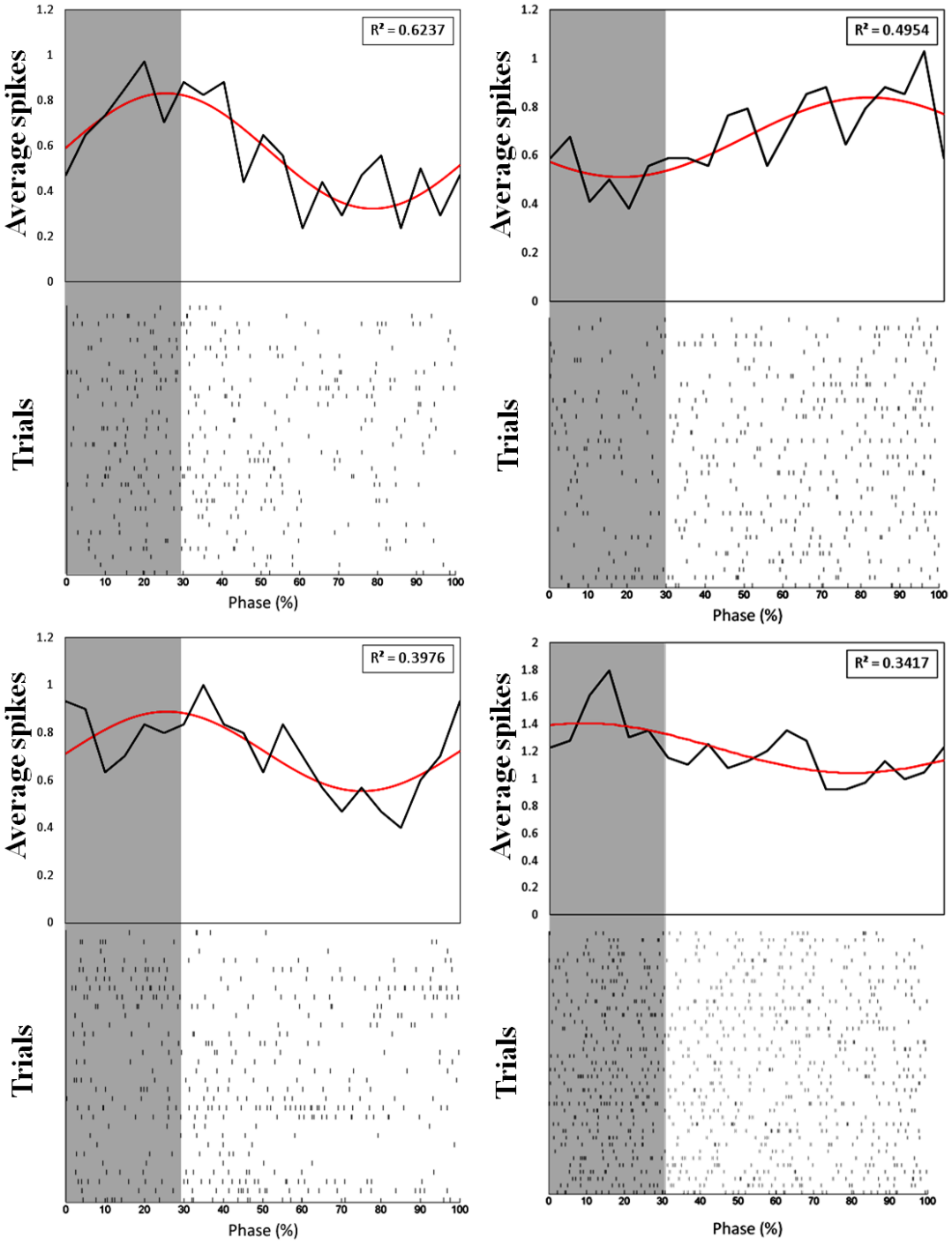

Figure 2.10 Average spikes per bin of four moderate units.

Summary and discussion

As described in this chapter, different locomotive states (standing/walking) can be identified from cortical recordings (as shown in Figure 2.5). The transition from one locomotive state to other locomotive state could also be identified from distinguished patterns of neural spikes rates (Figure 2.6 and 2.7). The step gait cycles could also be identified from these neural recordings (Figure 2.9 and 2.10). Thus, during the walking task, ample locomotive information could be extracted from cortical recordings in healthy subjects.

The current study on rats matches the previous findings of task-related modulation of cortical activity during motor tasks in cats (Drew, 1991; Beloozerova and Sirota, 1993; Drew et al., 1996). Additionally, it answers the question that different locomotive information (locomotive states, transitions and different gaits information) can be captured in parallel from hindlimb related area from rats' primary motor cortex.

To find out whether this information exist or not after spinal transection, experiment was designed and conducted as described in the following chapter.

CHAPTER 3: LOCOMOTION DETECTION IN SPINAL SUBJECTS

Background

All the studies in previous chapter utilized healthy animal subjects to parameterize the hindlimb related variables from cortical recordings. But, since the sensory inputs (both somatosense and proprioception) cannot reach to the brain after complete SCI, decoding cortical intention for locomotion may be very different for complete spinal transected subjects.

In a very recent rodent study, Manohar and colleagues demonstrated cortical neural modulation during a hindlimb related trained task that is available for neuroprosthetic control even after spinal cord transection (Manohar et al., 2012). In their study rats were trained to press a pedal using their hindlimb followed by an auditory cue (chime) to get water reward. The pedal was controlled in two modes: behavior control (BC) mode and neural control (NC) mode. In BC mode the rat gets the water reward with correct press in the pedal after listening the chime, whereas in NC mode the water reward was delivered by successful modulation in hindlimb area of sensory motor cortex (SMC) recorded by Teflon coated stainless steel microwire array. Similar with previous studies (Armstrong and Drew, 1984; Drew, 1988) it was found that SMC activities were modulated during hindlimb tasks. However, surprisingly, rats performed faster in NC mode compared to BC mode. Moreover, the duration and amplitude of press were shorter in NC mode compared to BC mode, while, more information was conveyed during NC mode (0.185±0.05 bits) than BC mode (0.105±0.03 bits).

It is crucial to reduce the dimensionality of the signal for successful and efficient prediction of kinematics for neurprosthetics. In the above study it was also

reported that Principal Component Analysis (PCA) dimensionality reduction was more efficient during NC mode (requires only 10% of PCs) compared with BC mode (requires 30% of PCs) for successful decoding of information. Increase of information by adding more PCs was significantly faster in NC compared to BC mode. Finally, a linear decoding algorithm was developed for successful reconstruction of hindlimb movement trajectory from this neural recording. It was also noted that the prediction of kinematics with feedback was better than without feedback.

The investigators tested the system in a motor imagery condition by removing the pedal, and later spinal transection, to find out the feasibility of using this neural information as neuroprosthetic controls for SCI subjects. No significant difference in neural modulation between NC with pedal and NC without pedal was found; however, signal to noise ratio (SNR) was improved in a later mode. After spinal transection (TX) the neural activities during the task reduced even below the BC mode. However, the average number of neurons recorded remained stable, but only 65% of them modulated during the imagery press task. This reduction resulted significant loss of information to 0.51±0.05 bits compared with BC mode (0.75±0.17 bits). But, relearning occurred in 10 to 15 days of training and information decoding increased to 0.76±0.03 bits in the last quarter of recording days. This impressive result supports the rationale of using cortical signal for lower-limb neuroprosthetic control after SCI.

The above study shows the significance of neural signals in the hindlimb motor area capable of generating significant information for neuroprosthetses controls even after complete spinal transection. However, for locomotion function, different information may be decoded form these cortical recordings. To answer the

additional question: whether the locomotive information (presented in the previous chapter) is still available after complete spinal transection or not, an experiment was designed to record the cortical signals from hindlimb cortical area in spinal rats (mid-thoracic) during forelimb locomotion task. The detail experimental methods are described in following sections.

Methods

Experimental subjects

Six healthy female Sprague Dawley rats weighing 250–350 g served as subjects in this study. All the subjects previously accomplished the treadmill locomotion task explained in the previous chapter. Subjects which have calm behavior during treadmill walking and good neural recordings were chosen for this new task.

Spinal transection

After the treadmill experiments, a second surgery was conducted to transect the spinal cord. Animals were pretreated subcutaneously with atropine sulphate (0.05 mg/kg, Sigma, USA) to restrain tracheal secretions. About 10 min after atropine injection, anaesthesia was induced intraperitoneally with 50 mg/kg pentobarbital sodium (54.7 mg/ml solution, Ceva Sante Animale Co., France) and maintained by supplemental doses (10 mg/kg/h, i.p.). The animal was mounted in a stereotaxic device and body temperature was controlled and maintained between 37 and 38°C by a homoeothermic system (Harvard Apparatus, USA). Laminectomy was made to expose the spinal cord at T9/T10 using a dental drill (Microtorque II, Ram Products Inc., USA). The spinal cord was transected with a microscissor. Care was taken not to damage the spinal arteries. Complete transection was confirmed by the absence of hindlimb movements in response to microstimulation in the cortex.

Stimulation electrodes implantation

Custom-made stimulation electrodes were placed in bilateral hindlimb muscles (gluteus superficialis, biceps femoris and semitendinosus), and the connecting wires were led subcutaneously to the head socket. The stimulation reference electrode was placed near the lumbar spine. The spinal opening and the skin incisions were sutured carefully.

Neural recording during forelimb locomotion

After 2–3 days of recovery from the second surgery, rats were placed on a treadmill with a harness. The hind part of the animal was lifted by a custom-made body weight support system, and only forelimb walking was permitted on the moving treadmill belt, shown in Figure 3.1. Neural signals were recorded using the same amplifier (A-M system differential AC Amplifier Model 1700, Sequim, WA) with band-pass filter (0.3–5 KHz). 10–20 recording sessions each of 1 min length were performed. The signals were digitised at 25 KHz using an Axon Digidata 1440 (Molecular Devices Co., Chicago, IL). Continuous video records were made using a video camera (Pleomax™, Samsung C&T Corporation, Korea).

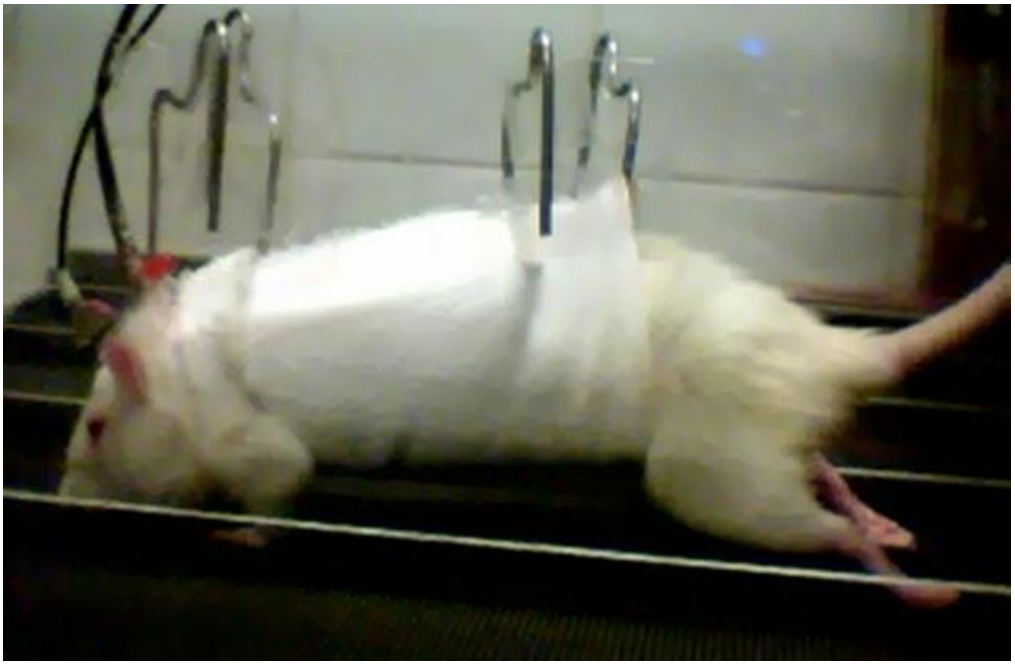

Figure 3.1 A spinal rat on a treadmill with custom body-weight support system.

Histology

After all experiments were completed, the animals were deeply anaesthetised intraperitoneally with 60 mg/kg pentobarbital sodium (54.7 mg/ml solution, Ceva Sante Animale Co., France). A constant direct current (approximately 100 μA) was delivered for about 1 min to each of the electrodes to produce heat markers at the implanted areas. The animals were then perfused transcardially with 300 ml 0.9% sodium chloride, followed by 300 ml of ice-cold 4% paraformaldehyde in 0.1 M phosphate buffer (pH 7.4). The brain was removed and post-fixed for 24 h in the same fixative. Coronal sections (50 μm) of the brain were sliced in cryostat microtome and Nissl staining was performed on slices covering the implant area of M1. Observation of these stained slices was carried out under a microscope (Nikon Corporation, Japan) and pictures were captured and stored on a computer.

Data analysis

Similar with previous experiment (explained in previous chapter) data were analyzed offline using custom-scripts written in MATLAB (MathWorks, MA, USA). Extracellular data were processed utilizing Axon Clampfit 10.0 (Molecular Devices Co., Chicago, IL). Neural spikes were detected and sorted using a MATLAB based open source electrophysiological data processing toolbox (Xiao-qin et al., 2011).

As in healthy subjects, neural activity was studied during the transition from stand-to walk (*Start*) and from walk-to-stand (*Stop*). For each unit, spikes were first binned into 50 ms and then a Perievent Time Histogram (PETH) was built by using the transition point from stand-to-walk as time 0. Activities from 1.5 sec to 1 sec before the transition time were used as baseline. For each 50 ms bin in this PETH, normalized firing rate values were calculated by subtracting the mean firing rate of the baseline and then by dividing by the standard deviation of the baseline. Finally, normalised firing rates of all *Start* and *Stop* units were generated, and units were grouped according to their firing rate patterns.

Raster plot and spikes time histogram were generated for each detected unit. The neural data were compared with the previous recording data of the healthy subjects for analyzing the relationship between before and after spinal transection. For step phase detection auto-correlation was accomplished on same detected unit before and after spinal transection. From -1.5 sec to +1.5 sec, the auto-correlation histogram was built for selected unit with 50 ms bin. Data analysis and graphing software, Origin (OriginLab Corporation), SPSS (IBM Corporation) and MATLAB were utilized along with Microsoft Office tools.

Results

Decoding walking intention after complete spinal transection

During the course of the experiment, previously identified single units dropped in almost all the subjects following the spinal cord transection. For each subject, around 7 to 10 single units were identified from these recordings (maximum one month after cortical implant). Figure 3.2 shows the average firing rate per cortical unit during the forelimb waking task with hindlimb suspended. The top panel illustrates the time raster of each single unit, while the bottom panel is the total spikes counts per 50 ms time bin. Walking started at 2.5 sec after standing while the treadmill started to move at 2.1 sec and stopped at 7.5 sec (shown by the dotted lines). The total recording was done for 10 sec. The firing rate was found generally high during walking.

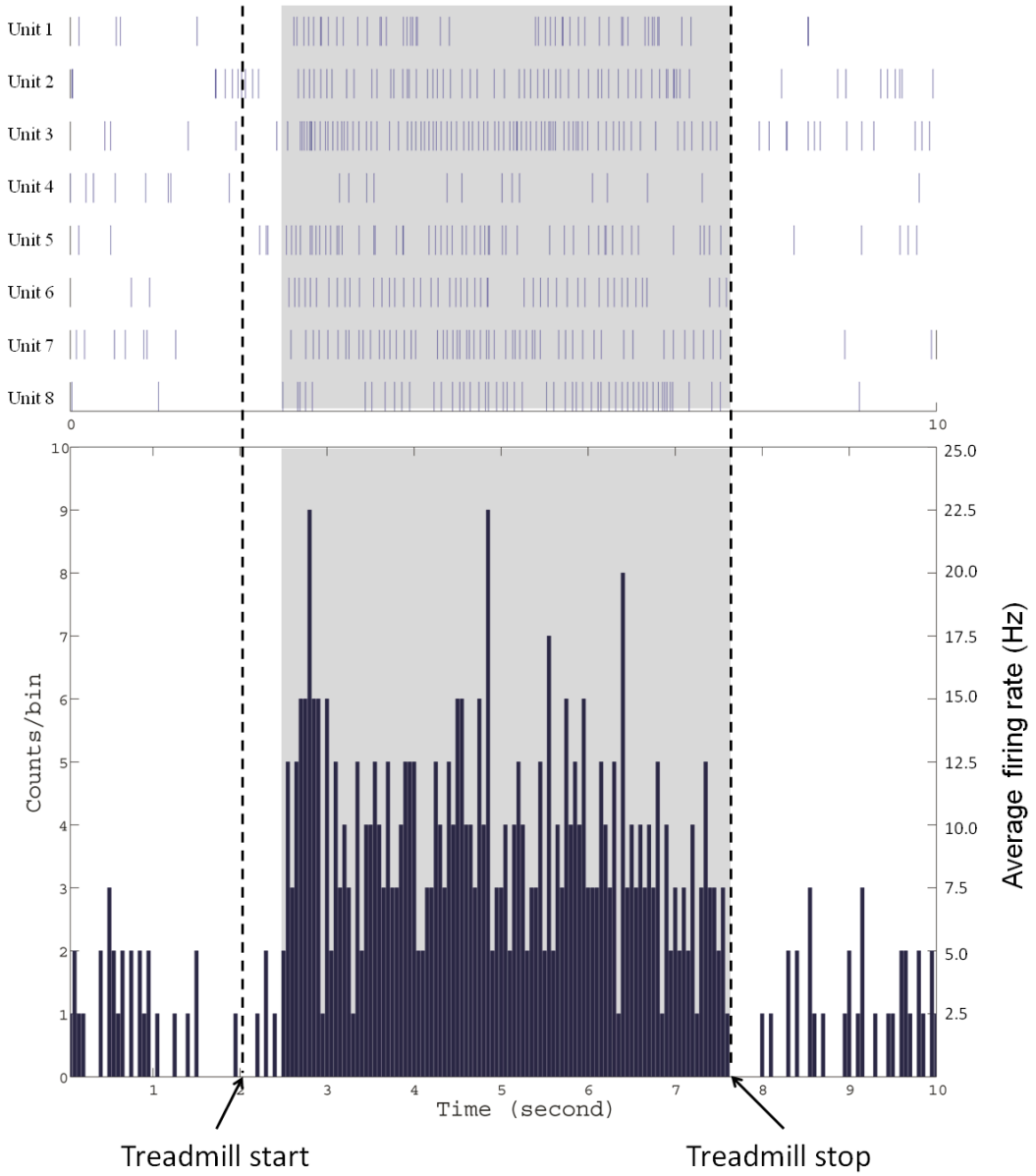

Figure 3.2 Average firing rate of cortical single unit during forelimb walking task. The gray area indicates the time of walking, while the rest white areas are standing. The dotted lines indicate the treadmill start and stop time.

Neuronal responses during stand-to-walk and walk-to-stand transition

The neural spike activities during the transition from stand-to-walk and walk-to-stand were studied during forelimb walking task after spinal transection similar with healthy subjects. Similarly, for stand-to-walk transition the units are named as *Start* units, while, walk-to-stand units are named as *Stop* units. Firing rates patterns of all

Start and *Stop* units were analyzed. After normalization a total of three groups of *Start* units (according to their firing rate patterns) were identified, as shown in Figure 3.3.

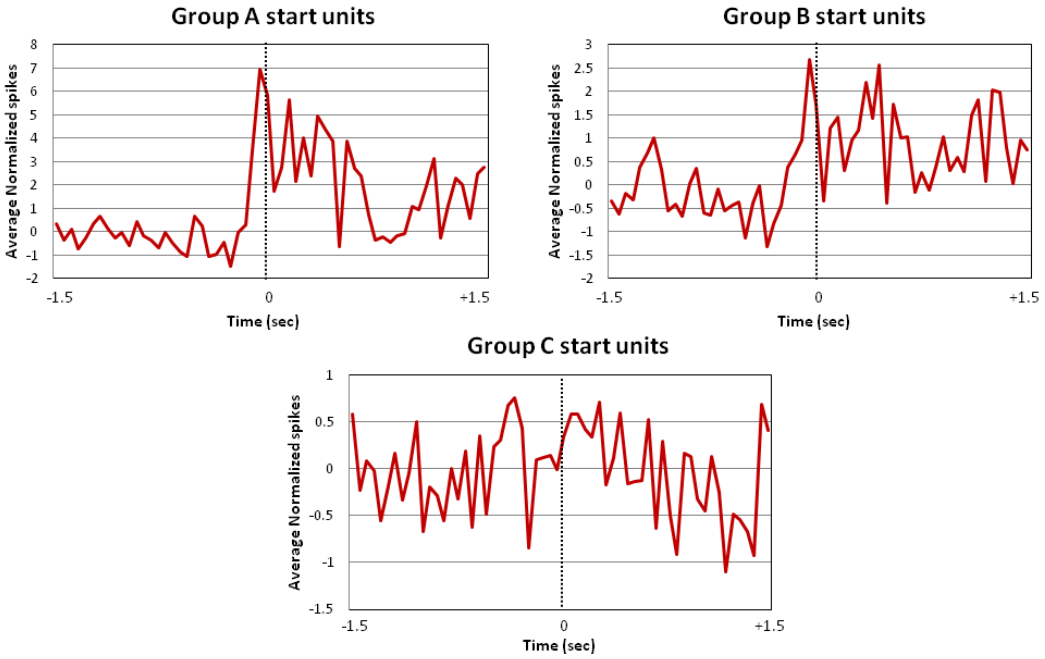

Figure 3.3 Average normalized spikes rates during stand-to-walk transition for three groups of neural units. The horizontal dotted line indicates the walking activation time.

Group A *Start* units: 30% single units are grouped into this category. Their firing rate patterns exhibited a positive pick at the onset of forelimb walking.

Group B *Start* units: 30% single units are grouped into this category. Their firing rate patterns signified with a slight increase of baseline firing rates from the onset of walking.

Group C *Start* units: 40% single units are grouped into this category. No distinguishable firing rate patterns could be identified for this category of neurons during this task.

Similarly, walk-to-stand transition, that is, *Stop* units were identified and grouped into two major categories for the forelimb walking talk of spinal subjects, as shown in Figure 3.4.

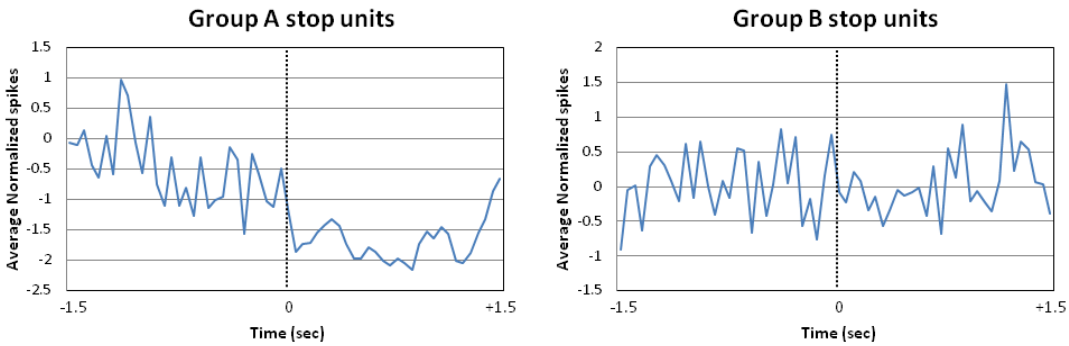

Figure 3.4 Average normalized spikes rates during walk-to-stand transition for two groups of neural units. The horizontal dotted line indicates the stopping from walking.

Group A *Stop* units: 70% single units are grouped into this category. Their firing rate patterns signified with decreasing baseline firing rates from the onset of standing.

Group B *Stop* units: 30% single units are grouped into this category. No distinguishable firing rates pattern could be identified for this category of neurons during this task.

Comparison of neural activities before and after spinal transection

A comparison of total neural units(N = 80) firings before and after spinal transection was accomplished and found significant ($p < 0.01$; two-paired t-test), as illustrated in Figure 3.5. It was found that the average cortical firings were generally high in healthy subjects (77 Hz during standing and 137 Hz during walking). These numbers decreased significantly (14 Hz during forelimb standing and 77 Hz during forelimb walking) after spinal transection. However, it was still possible to detect locomotive states (standing or walking) form these recordings.

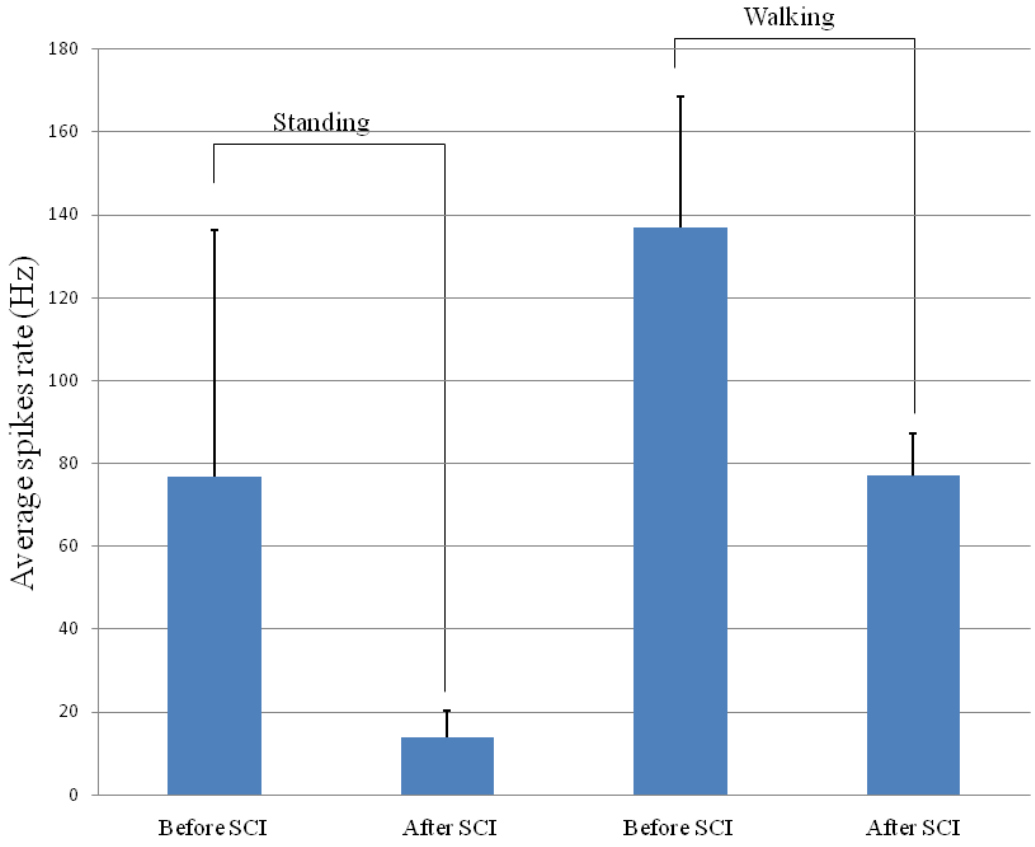

Figure 3.5 Comparison of neural spikes rate before and after spinal transection.

Histological confirmation of the electrodes placements in hindlimb area of rats' primary motor cortex is shown in Figure 3.6. The rostral electrodes are more lateral compared to the caurdal electrode implants, as the limb representation in motor cortex of rat is organized in same manner (as shown previously in Figure 2.4). Solid arrows indicate the electrode traces in the histological slides. According to the slides, the electrodes depths confirm layer-V/layer-VI implantations.

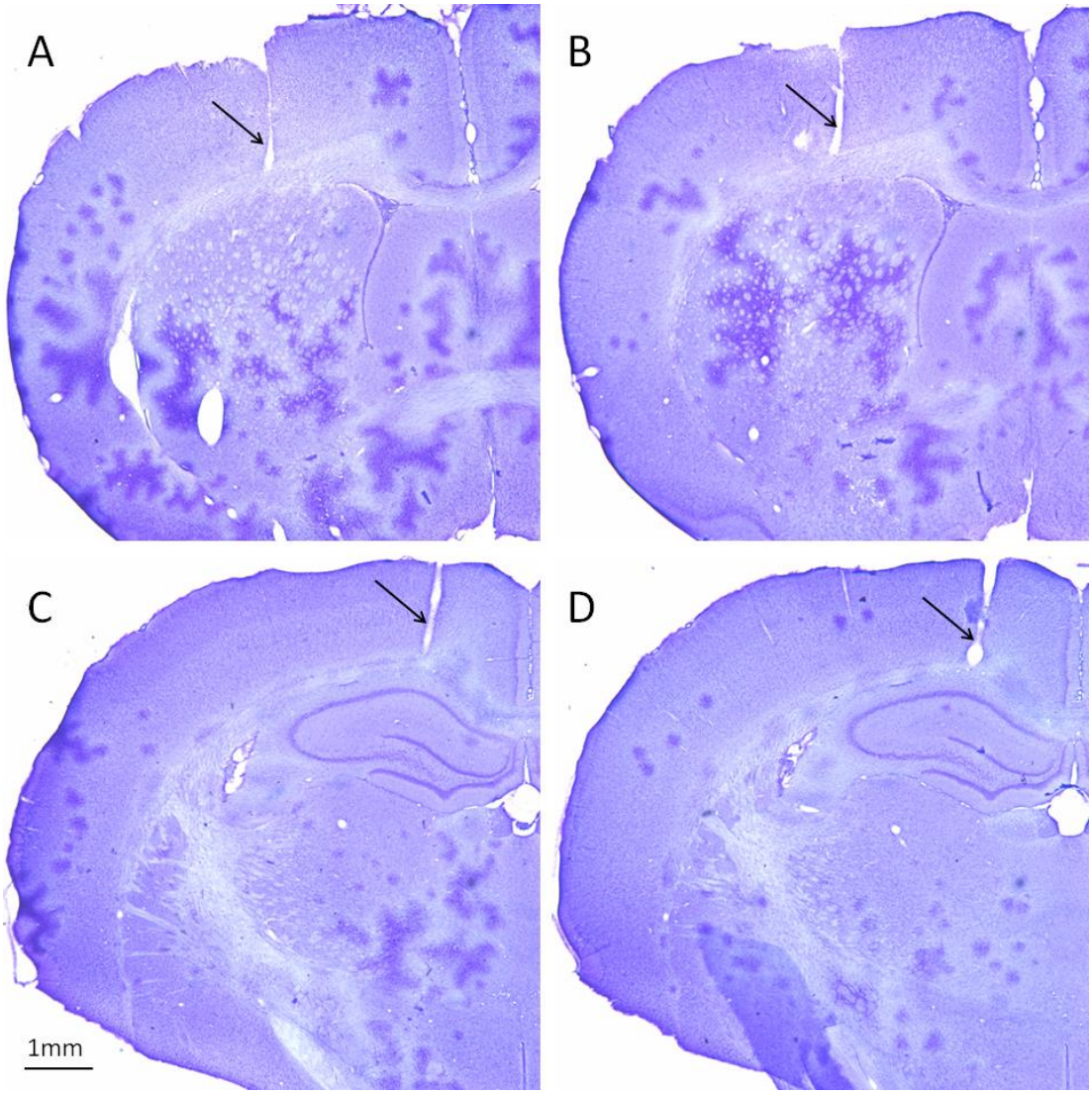

Figure 3.6 Electrodes locations (indicated by the arrows) in brain slides of subjects (A-B) rostral implants and, (C-D) caudal implants.

Summary and discussion

As described in this chapter, different locomotive states (standing/walking) can still be identified from the cortical recordings (Figure 3.2 and 3.5), even after complete spinal transection. The transition from one locomotive state to other locomotive state could also be identified from distinguished patterns of neural spike rates (Figure 3.3 and 3.4). A recent study may explain this finding as showed that different sources of locomotion (controllers) are located in spinal cord rather than in the cortex of cats (Zelenin et al., 2011). After paralyzing spinal transection, the efferent copy from these limb controllers (spinal network) could not reach to the brain (Orlovskii et al., 1999). However, locomotive states (standing/walking) could still be decoded from these recordings and thus could be utilized for neurosprostheses controls.

The following chapters describe designing a novel system to utilize this real-time neural information for the restoration of hindlimb locomotion for spinal rats.

CHAPTER 4: DEVELOPMENT OF AN ELECTRONIC SPINAL BRIDGE

Overall system architecture

An electronic spinal bridge, called "Motolink" was designed and developed to provide a connection between the primary motor cortex (M1) and the hindlimb muscles after spinal injury (Figure 4.1). The circuit consists of three major parts: 1) a head-mountable, multichannel, neural recording amplifier, 2) a real-time neural signal processor, and 3) a controlled electrical stimulation circuit. This circuit filtered and amplified the neural information, then processed this information in real-time to generate trigger signals for the stimulation circuit.

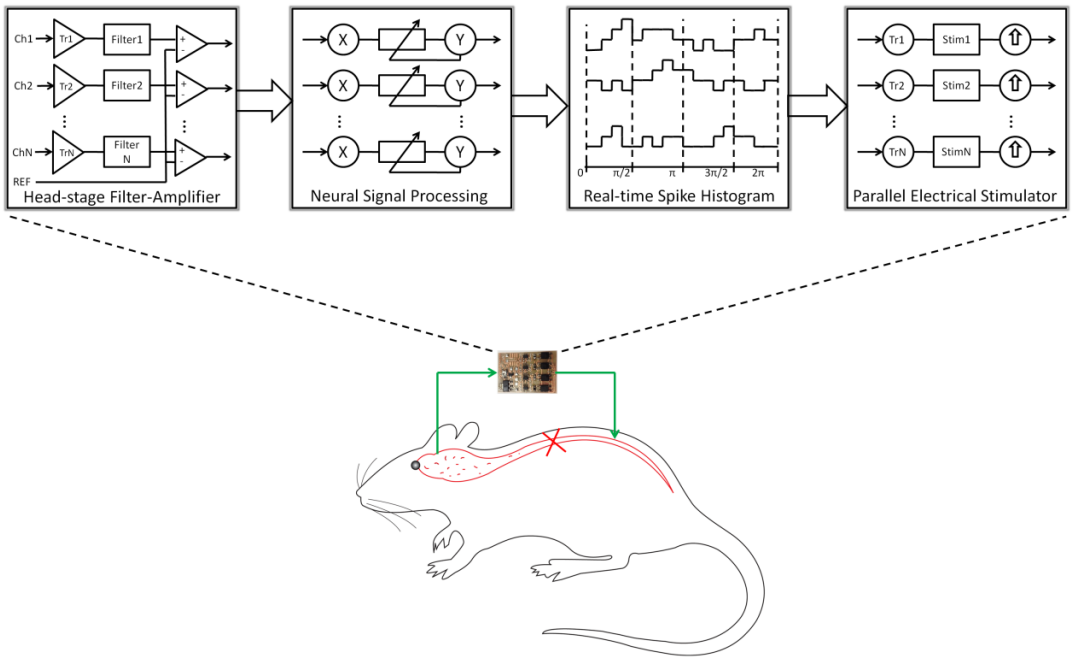

Figure 4.1 A conceptual diagram with detail system architecture of the "Motolink" hardware. The cross on the rat schematic indicates complete spinal transection. The green arrows show the input and output of "Motolink" circuit that allows neural signals to bypass the spinal transection

Multichannel neural recording amplifier

The analogue front-end circuit is one of the most critical parts of any electrophysiology system (Heuningen et al., 1984). Due to space limitations, we considered Commercial Off-The-Shelf integrated circuits with small foot-prints. The front-end consisted of two main stages: the preamplifier stage, built with an instrumentation amplifier (IA), and a second-order Sallen-key filter amplifier, constructed with a low-noise operation amplifier. Figure 4.2 shows the schematic diagram of the amplifier circuit.

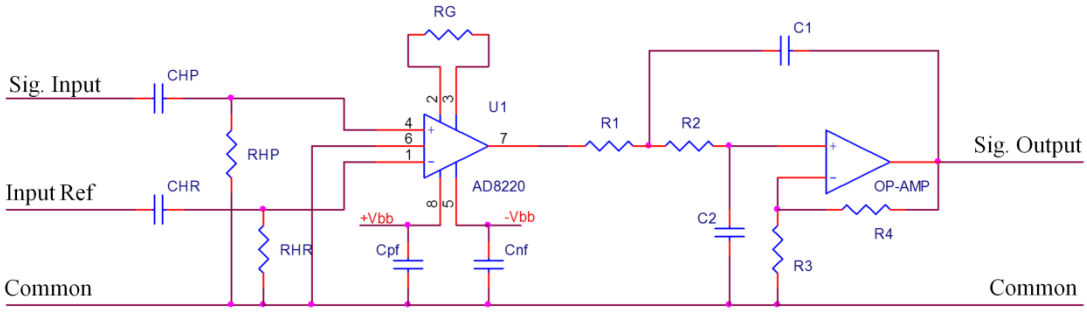

Figure 4.2 Schematic diagram of the neural signal recording amplifier. Only one channel out of eight been presented in the schematic.

For successful recording of neural spikes, it is important to keep the noise level as low as possible (Wattanapanitch et al., 2007). Noise is an inherent characteristic of electrical circuits and is associated with the random nature of the movements of charge carriers (Motchenbacher and Connelly, 1993). When measuring very small signals with an IA, it is important to consider the different sources of noise to choose the correct amplifier. Noise is represented in terms of root mean square (RMS) power where all noise sources are added together in a root sum of squares fashion (Jung, 2005), as follows:

$$\text{Total RTI (refer-to-input) noise (nV/}\sqrt{\text{Hz}}) = \sqrt{(e_{ns})^2 + (e_{ni})^2 + (e_{no}/G)^2 + (i_{ni} * R_S)^2}$$

Here, e_{ns} is the source resistance noise, e_{no} and e_{ni} are the voltage noises, i_{ni} is the current noise of an instrumentation amplifier.

After researching the availability of COTS instrumentation amplifiers, we selected two IA that have most suitable performances for our requirements. One of them is INA116 (Texas Instruments, Dallas, TX) and the other is AD8220 (Analog Devices, Norwood, MA). Due to size advantages we had chosen AD8220 IA for our designs. After putting different noise values for AD5220 IA from the datasheet:

$$\text{Total RTI noise} = \sqrt{(e_{ns})^2 + (e_{ni})^2 + (e_{no}/G)^2 + (i_{ni} * R_S)^2}$$

$$= \sqrt{(128.5)^2 + (14)^2 + (90/1000)^2 + (1)^2}$$

Total RTI noise = 129.26 nV/$\sqrt{Hz}$

This is nearly identical to the noise with only the source resistance. The total RMS noise can be limited by filtering after the IA to reduce the bandwidth as much as possible without distorting the signal of interest. Noise at these later stages is less significant because the RTI noise value is divided by the gain of the IA. In our design we obtained an effective noise bandwidth from 300 Hz to 5 KHz. For our two-pole low-pass filter with a cut-off frequency (f_C) of 5 KHz, this resulted in an effective noise bandwidth of 1.11*f_C. We used this approximation to calculate overall RMS voltage noise of the system as follows:

RMS voltage noise = 129.26 nV/$\sqrt{Hz} * \sqrt{5000 - 300} * 1.11$ = 9.84 µV

When recorded by microwire arrays, the amplitude of extracellular spikes is generally 100–300 µV (Nicolelis, 2007). Hence, 10 µV instrument noise is sufficient for the recording of neural spike activities. The complete printed circuit board of the analogue front-end circuit (Figure 4.3A) was small enough to be mounted on the head of a rat. Figure 4.3B shows the frequency response of the amplifier. The pass-band gain of the circuit was just over 80 dB.

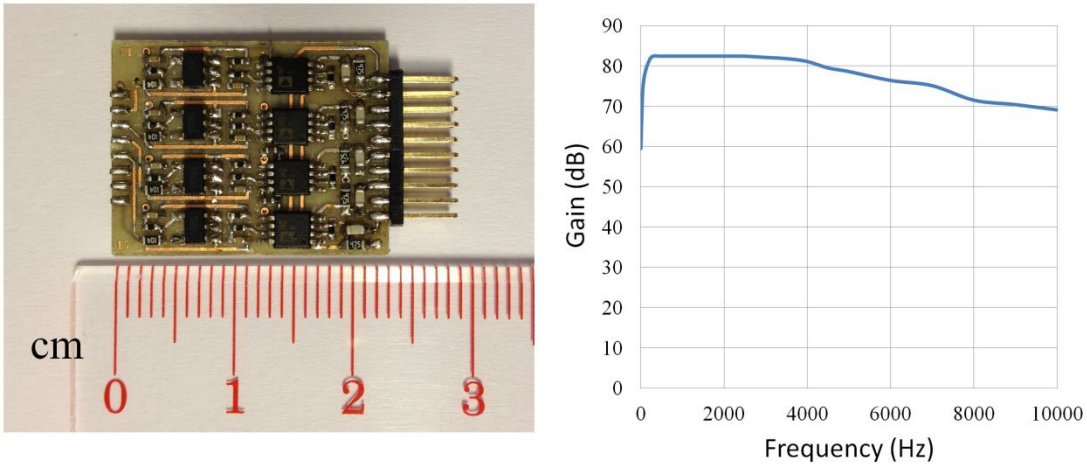

Figure 4.3 Complete circuit of a head-mountable 8 channel neural recording amplifier: (A) complete circuit board, and (B) frequency response of one channel.

Neural signal processing

A neural signal processing system was designed to decode the locomotive information contained within the neural signals in real-time. The system was composed of two major parts: an online spike detection circuit and a signal processor unit (Figure 4.4).

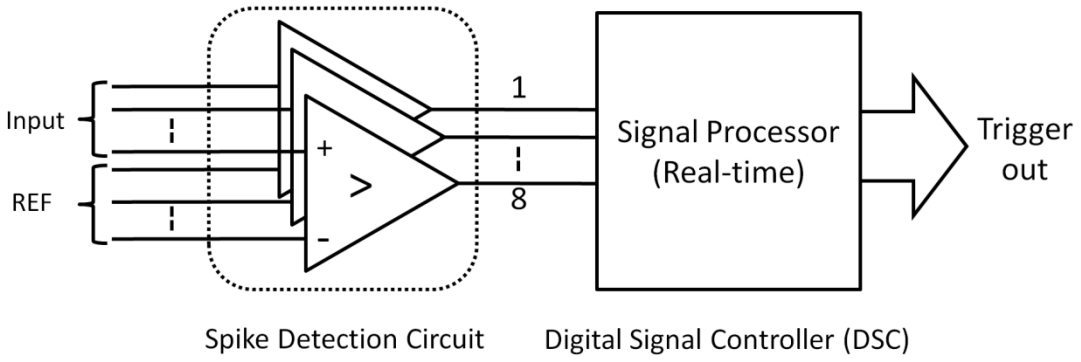

Figure 4.4 Neural signal detection and processing circuit. After online spike detection from analog signals, spike processing is done by a signal processor to generate trigger signals for the electrical stimulator.

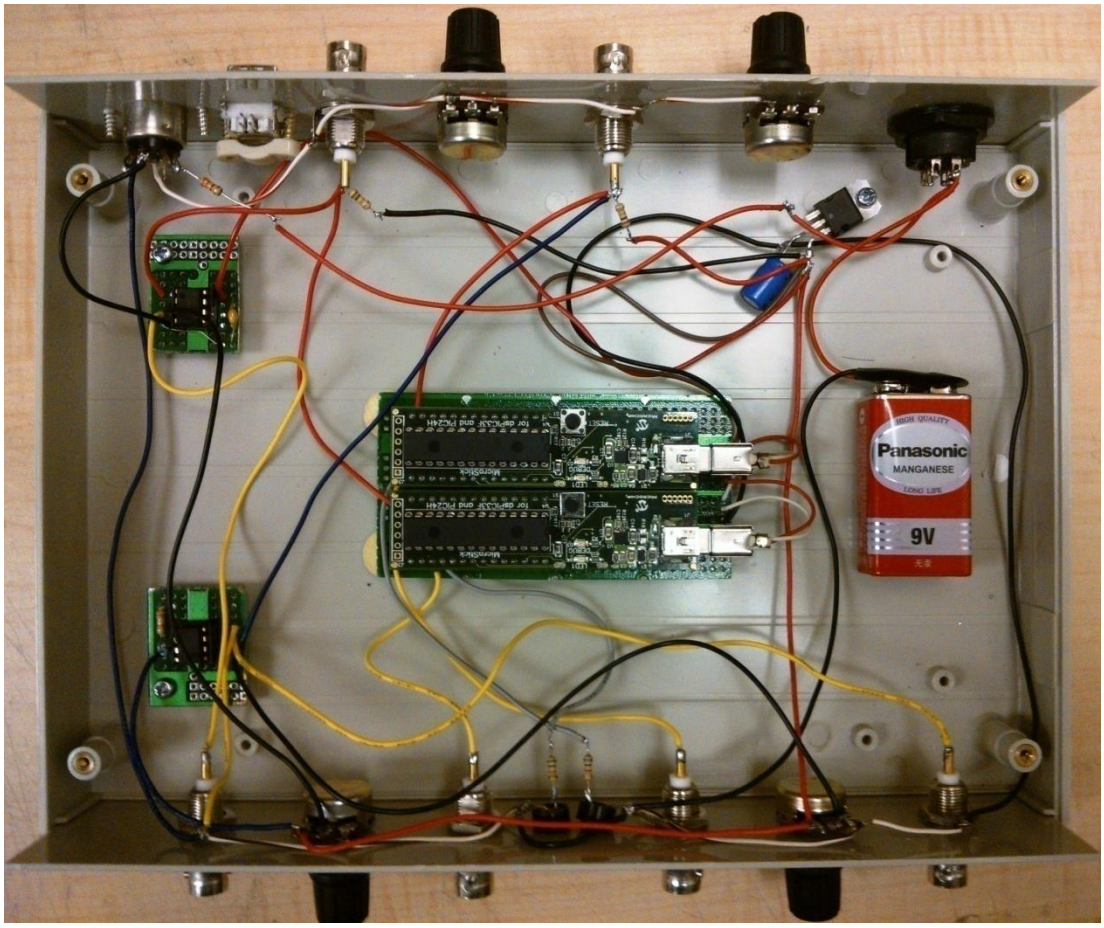

Figure 4.5 Complete circuit for neural signal detection and processing with variable thresholding options. The circuit is entirely powered by a single 9 volt rechargeable battery.

Different online spike detection algorithms were installed and tested on this system. Among them, the median value spike threshold method was the best similar found in previous study (Gibson et al., 2008). The threshold for each channel was determined in a spike training phase according to the following equation:

$$\text{Threshold} = 4\sigma N, \qquad \text{where } \sigma N = \text{median } \{\frac{|x(n)|}{0.6745}\}$$

The processing of neural signals was accomplished by a 16-bit digital signal controller that was fast enough to process several neural channels simultaneously. Large on-chip memory permitted spike counts to be made in 100 ms bins. The bin

was moved every 20 ms to generate a smooth spike histogram, as shown by the program flowchart in Figure 4.6.

At the start of spike training phase, the processor initialized on-chip timers, counters and reset the bins. During the training phase, the system calculated the average spontaneous spike counts to determine a threshold for each bin. In parallel, the automatic spike detector circuit provided the time stamp for the neural processor to count the spikes in allocated bin. Every 20 ms, the number of spikes in the bin was compared with the reference spike number, and if the number of spikes in the bin exceeded the reference spike number a trigger pulse was generated for the electrical stimulator circuit.

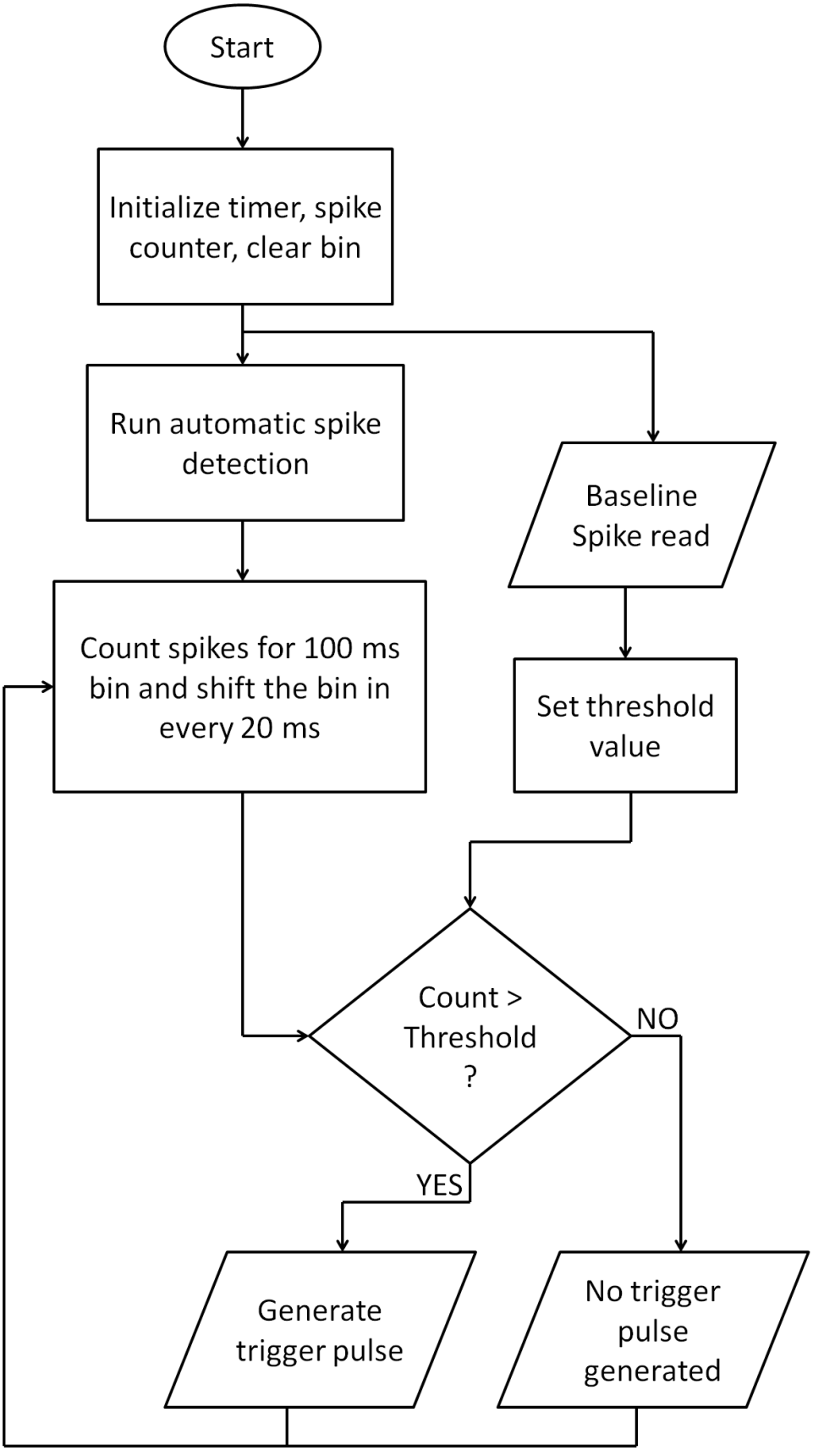

Figure 4.6 Neural signal processing algorithm flow chat.

The simplified code for the above algorithm (written in C programming language) is given as follow:

```
// Add supports for DSC Peripheral library functions and macros
#include <plib.h>

// Global variable
int Spike_Counter;

// Configuration Bits
#pragma config FNOSC    = PRIPLL        // Oscillator Selection

// Let compile time pre-processor calculate the CORE_TICK_PERIOD
#define SYS_FREQ                    (80000000)
#define TOGGLES_PER_SEC             1
#define CORE_TICK_RATE          (SYS_FREQ/2/TOGGLES_PER_SEC)


// timer interrupt application
int main (void)
{
   // Initialize global counter
   Spike_Counter = 0;

   //Initialize the DB_UTILS IO channel
   DBINIT();
   // enable device multi-vector interrupts
   INTEnableSystemMultiVectoredInt();

   // Configure the device for maximum performance, but do not change the PBDIV clock divisor.
   SYSTEMConfig(SYS_FREQ, SYS_CFG_WAIT_STATES | SYS_CFG_PCACHE);
   // configure the core timer roll-over rate (100msec)
   OpenCoreTimer(CORE_TICK_RATE);
   // set up the core timer interrupt with a priority of 2 and zero sub-priority
   mConfigIntCoreTimer((CT_INT_ON | CT_INT_PRIOR_2 | CT_INT_SUB_PRIOR_0));
   // configure PORTD = trigger output
   mPORTDSetPinsDigitalOut(BIT_0);
   // configure PORTB = signal input
   PORTSetIn(IOPORT_B);

   While (1)
         {
                  // wait
                  While (PORTDbits.RD13 == 1)
                  {
                           mPORTDRead();
                  }
                  mPORTDToggleBits(BIT_1);
                  // wait
                  While (PORTDbits.RD13 == 0)
                  {
                           mPORTDRead();
                  }
                  mPORTDToggleBits(BIT_1);

                  Spike_Counter++;
         }
}
```

```
// interrupt routine
void __ISR(_CORE_TIMER_VECTOR, ipl2) CoreTimerHandler (void)
{
        // Initialize
        int z;

        // Condition check
        if(Spike_Counter>10)
        {
                // send a pulse
                mPORTDToggleBits(BIT_2);
                for(z=0;z++;z>10000);
                mPORTDToggleBits(BIT_2);
        }
        Spike_Counter = 0;

   // .. Toggle the LED
   mPORTDToggleBits(BIT_0);

   // update the period
   UpdateCoreTimer(CORE_TICK_RATE);

   // clear the interrupt flag
   mCTClearIntFlag();
}
```

Controlled electrical stimulation

A voltage pulse stimulator (Master-8 A. M. P. I., Israel) was used to generate biphasic electrical stimulation pulses from the external trigger of the neural signal processing system, shown in Figure 4.7. To find the optimum stimulation parameters the amplitude, width and number of the stimulation pulses were varied in anesthetized subjects. During the experiment sessions these parameters were kept constant (300 µS pulse width, 100 µS inter-pulse interval and 500 µS pulse delay) except only the amplitude. The amplitude was increased progressively each day to generated hindlimb movement from the stimulation. To isolate the recording system from the electrical stimulation current isolator (Harvard Apparatus, USA) was used for each stimulation channel.

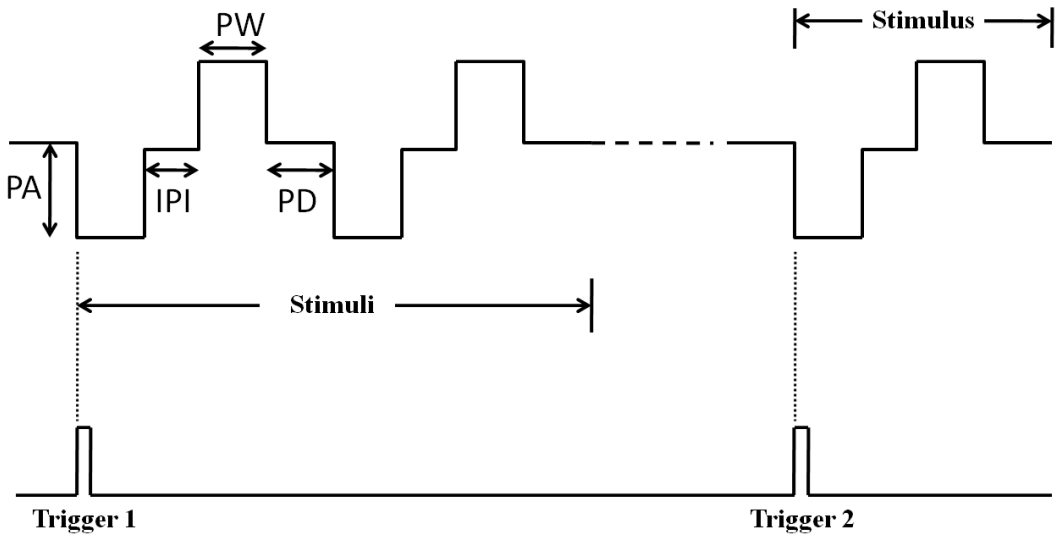

Figure 4.7 Biphasic electrical stimulation generated from the trigger signals. PA: pulse amplitude, PW: pulse width, IPI: inter-pulse interval, PD: pulse delay for one stimulus. The stimulus number was set between 1 to 5 in different experimental subjects' requirements.

CHAPTER 5: CORTICALLY TRIGGERED ELECTRICAL STIMULATION FOR RESTORATION OF LOCOMOTION

Predicting step cycles from cortical recording

The developed neuroprosthetic device "Motolink" (discussed in the previous chapter) is capable of multichannel neural signals recording, processing and generating trigger signals for the electrical stimulator. To test the performance of "Motolink" hardware, offline emulation was performed for a single channel cortical recording (Figure 5.1).

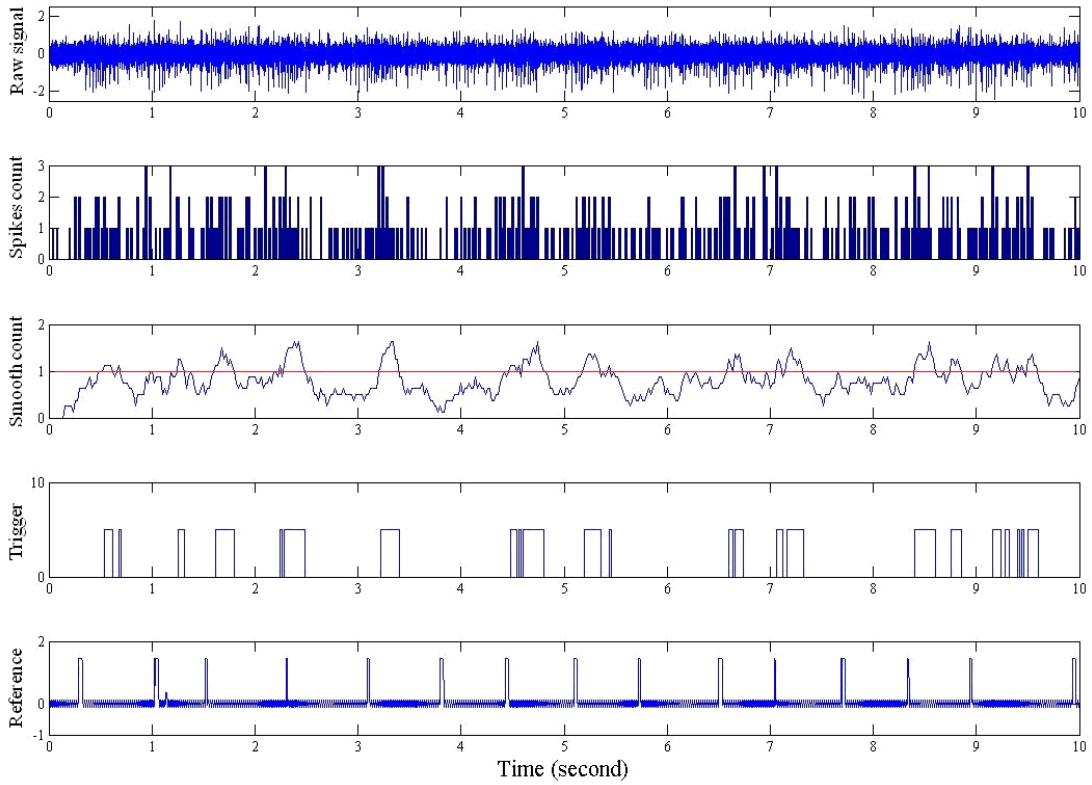

Figure 5.1 Algorithm emulation of online step cycles prediction from one channel cortical recording. Y-axis in each panel represents voltage. A raw neural signal recorded from one cortical electrode is shown in the first panel. The signal was processed to generate spike histogram, and then smoothed. The smoothed signal was then thresholded (shown by red line) to generate the voltage triggers. The final panel shows the original reference signal from the tilt sensor during walking task.

The neural detection and processing circuit (Figure 4.4) processed a raw neural signal that had been recorded from one cortical electrode during gait of a healthy subject, and generated a spike histogram in 50 ms bins (Figure 5.1, panel two). After smoothing (moving average) and thresholding (Figure 5.1, panel three), emulated triggers were generated (Figure 10; panel four). The predicted step times were calculated, and compared to the actual step times observed during gait (Figure 5.1, panel five). The mean time delay of predicted steps from the actual steps was 113.41 ms (Standard Deviation 92.13 ms). There were three miss-triggers, whereby a step occurred but was not predicted, and few false-triggers, whereby a step was predicted but did not occur. False-triggers were further handled by safety routine in the algorithm (by adding additional 50 ms delay following the negative edge of each trigger).

Triggering electrical stimulation from direct cortical recording

To test the performance of "Motolink" in real-time, the hardware was connected to the head socket of a spinal rat. Figure 5.2 shows the neural recordings from seven cortical electrodes and two channels of spike detections (from channels two and six) obtained while the animal was resting. These recordings were used to set the baseline thresholds for online spike detection during the forelimb locomotion task.

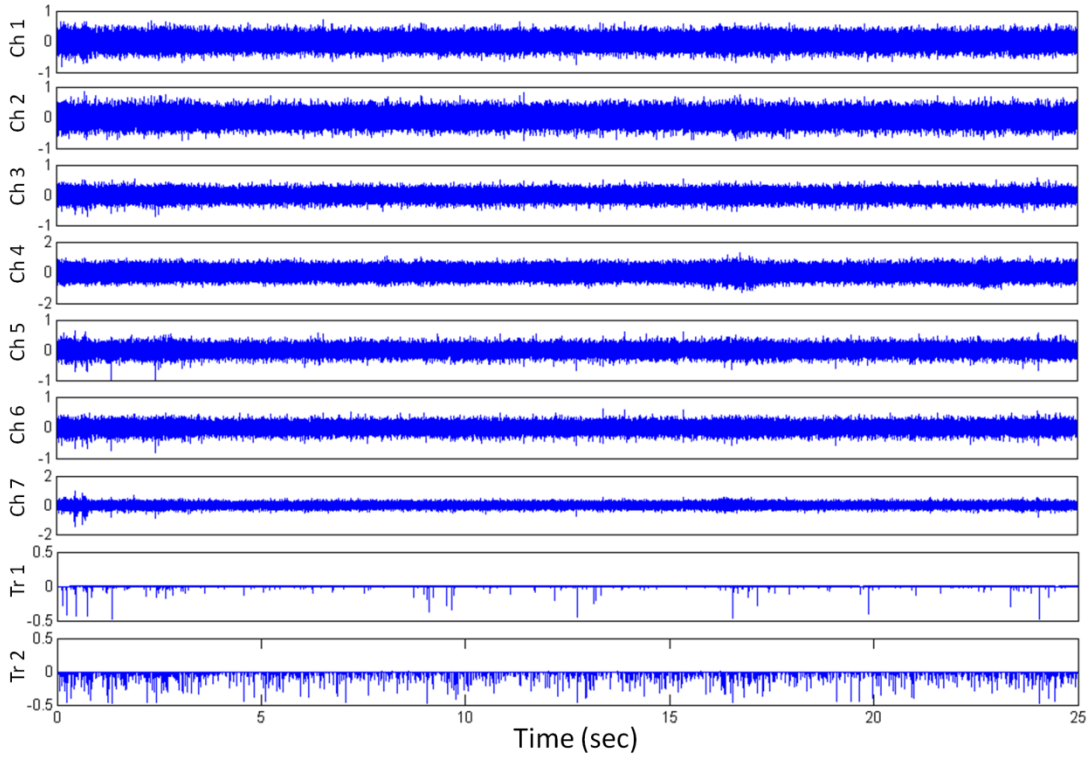

Figure 5.2 Online triggering from spontaneous neural activities during quiet standing. Y-axis in each panel represents voltage. First seven channels (Ch1 to Ch7) show the neural recordings from seven cortical electrodes. Final two rows (Tr1 and Tr2) show two channels of trigger sources (from Ch2 and Ch6).

After setting the threshold values, the "Motolink" hardware successfully generated electrical stimulations. Figure 5.3 shows a single channel cortical recording, spike detection, and generation of biphasic electrical stimulation from a freely roaming rat. The detected spikes had higher frequency modulation during walking (10^{th} to 20^{th} sec as well as 30^{th} sec), and also reflected in the electrical stimulation (Figure 5.3; last panel).

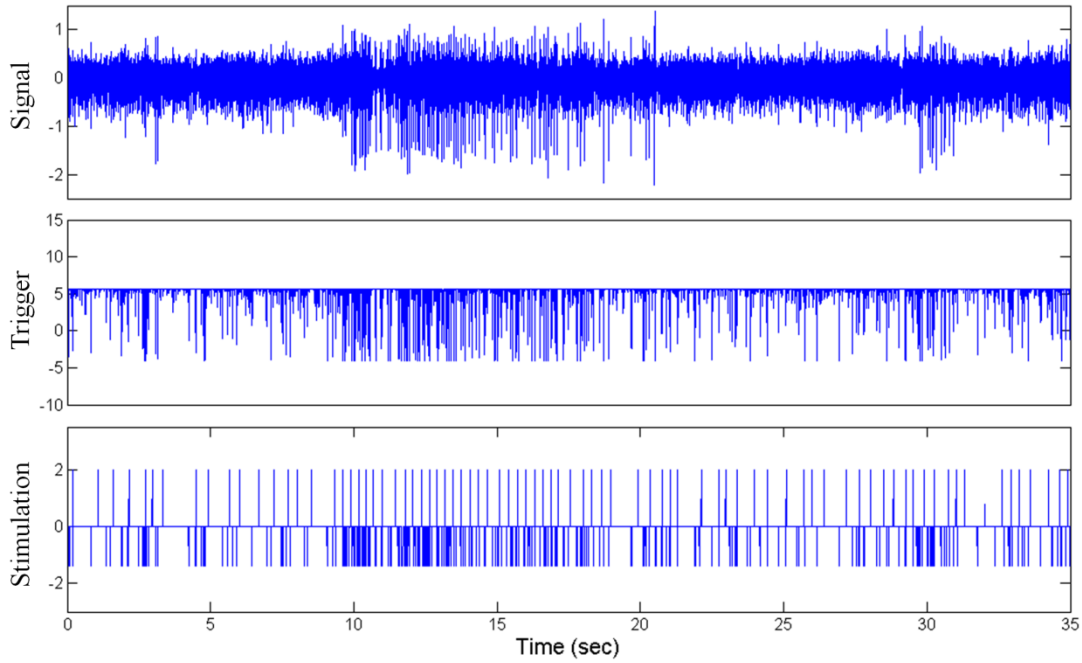

Figure 5.3 One channel neural signal recording (panel one), real-time spike detection (panel two) and generation of electrical stimulation (panel three) for a freely roaming rat. Y-axis in each panel represents voltage in volt.

Finally, the "Motolink" hardware was tested in the spinalised rats (n = 6) while they were performing the forelimb walking task on a moving treadmill belt with suspended hindquarters. The cortical signals recorded from the hindlimb cortical area during forelimb walking were used to control electrical stimulation of the hindlimb muscles. Stimulation-induced contraction of the hindlimb muscles occurred during the forelimb movements (Supplementary video 2). Figure 5.4 illustrates the raw neural signals and trigger signals generated by the "Motolink" hardware. Two trigger signals (Tr1 and Tr2) were generated from two cortical recording channels (Ch1 and Ch2) for stimulating both hindlimbs. Thus, for the first time, a brain-machine-muscle interface was established for the restoration of hindlimb locomotion in spinal rats.

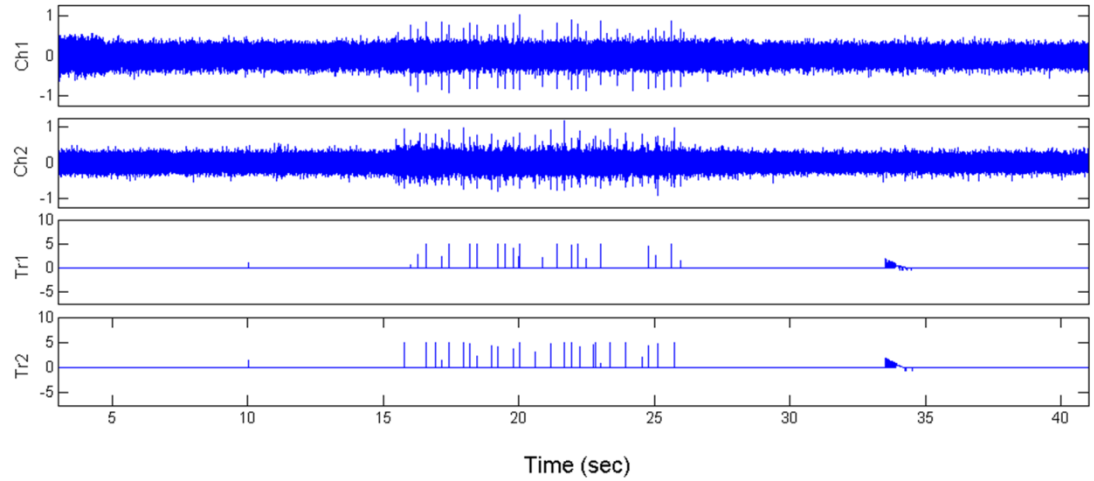

Figure 5.4 Electrical stimulation of paralysed hindlimbs from direct cortical recordings to restore movements. The data in this figure refer to Supplementary Video 2. Y-axis in each panel represents voltage. The stimulator was turned on at 10th sec and turned off at 34th sec, and the treadmill was running from 15.5th sec to 26th sec. Two hindlimb triggers (Tr1 and Tr2) were generated from two cortical recording channels (Ch1 and Ch2).

Summary and discussion

As described in this chapter, the developed neuroprosthetic device "Motolink" records cortical neural signal, processes the signal in real-time and generates electrical stimulations for hindlimb movements in spinal rats. The prediction accuracy of steps in healthy subjects was measured 79% (11 out of 14 steps were successfully identified with a mean time delay of predicted steps from the actual steps of 113.41 ms; standard deviation 92.13 ms). However, in spinal subjects as most of the step gait information disappeared after spinal transection, the "Motolink" hardware only successfully predicts the transition and locomotive states (standing/walking). From the supplementary video 2, it was found that the stimulation only occurred during the forelimb walking. This illustrates the potential of using such device for paraplegics; although, there are rooms of improvements required before final application. At the moment the stimulation is from one cortical recording to one electrical stimulation channel. But locomotion requires multiple muscles activation and coordination (Inman, 1966; Dietz et al., 2001). A preprogrammed stimulator with predefined stimulation pattern would improve the functionality (Pedotti et al., 1992; Graupe, 2002; Xie et al., 2009).

Most of the lower level locomotive functions are accomplished by the spinal pattern generators (Orlovskii et al., 1999). Currently, the "Motolink" hardware does not have such function. But the device has space to input such function. It has multichannel analogue and digital inputs and outputs. The core of the device is a 16 bit Digital Signal Controller (DSC) running at 40 MHz speed with 32 Kbytes program memory and 4 Kbytes working memory. The device can work as a core of Central Pattern Generator (CPG) to send preprogrammed stimulation patterns to the limbs to mimic walking. For functional restoration of walking the stimulation should

be frequency modulated with time varying switching mechanism between different stimulation channels as the real walking requires activation of different muscles at very accurate time differences (Ivanenko et al., 2005).

CHAPTER 6: CONCLUSIONS AND FUTURE RESEARCH DIRECTIONS

Conclusions

The growing number of Spinal Cord Injury (SCI) has a large impact on both individuals' and society. Roughly half of the SCI population is paraplegics (Matthew, 2002); hence, improving the quality of life for paraplegic patients will be valuable to individuals' and also extremely beneficial to the society, both socially and financially. There is no complete cure for severe SCI yet (Freund et al., 2011). The recovery of standing and walking functions after the injury strongly depends on type, location and the severity level of the spinal cord lesion (Hubli and Dietz, 2013). For incomplete injuries, it has already been established that extensive physical therapy and locomotor training help to regain motor functions including standing and walking; however, the same intervention failed to provide significant improvements for motor complete SCI paraplegics (Behrman and Harkema, 2000; Rossignol and Frigon, 2011). Combining epidural spinal cord stimulation along with these rehabilitation therapies, patients would likely regain some motor functions, shown in one pilot study (Harkema et al., 2011). However, extensive clinical trials are needed to find out the exact effect of this new intervention. Even if spinal stimulation restores some motor function, it lacks the natural cortical "*intent"* to initiate or stop the stimulation. Similar problem exists for Functional Electrical Stimulation (FES) systems (Boord et al., 2004; Xie et al., 2009). A hand switch driven stimulation is very unnatural compared with functional locomotion.

With the development of microscale neural recording and stimulation we believe cortical control of electrical stimulation would be significant for restoring lower-limb motor functions in motor complete SCI paraplegics (a conceptual

diagram of such a system is shown in the Chapter 1). The electrical stimulator system is similar to those in heart pace maker (ideally implanted into the body). The stimulator is linked to the cortical recordings. Neural intention can be captured by microelectrode arrays from lower-limb primary motor area (M1). This neural "*intent*" is decoded by advance computer algorithms to trigger electrical stimulation that generate movements. A very recent study of such a system demonstrated the restoration of upper-limb movements in a monkey with cervical spinal cord injury (Nishimura et al., 2013).

To verify the concept of lower-limb artificial spinal bridge, laboratory rats were used as SCI model in this research study. As discussed in Chapter 2, the results on healthy subjects demonstrated that different locomotive states (standing/walking) could be identified from multiunit neural spikes of cortical recordings. The transition from one locomotive state to the other locomotive state (standing-to-walking and walking-to-standing) could also be identified from distinguished patterns of these neural spikes rates. The states of step gait cycles (stance phase and swing phase) could also be identified from these neural recordings. Thus, during walking, ample locomotive information could be extracted from cortical recordings in healthy subjects. Current experimental data on rats supports the previous findings of cortical modulation during task related motor functions in cats (Drew, 1991; Beloozerova and Sirota, 1993; Drew et al., 1996). Additionally, the study showed that different locomotive information (locomotive states, state transitions and different gait information) could be captured in parallel form rats' hindlimb area of primary motor cortex.

In order to determine whether this neural information exists or not after complete spinal transection, experiments were conducted on spinal subjects (mid-

thoracic). As discussed in Chapter 3, it was found that though the spikes activities decreased significantly ($p < 0.01$; two-paired t-test) after complete spinal transection, different locomotive states (standing and walking) could still be identified from these cortical recordings. Similar to the healthy subjects, transition from one locomotive state to the other locomotive state could also be identified from distinguished patterns of neural spikes rates. But, the detail locomotive information such as different step gait phases (stance or swing phase) modulation mostly disappeared from these cortical recordings after spinal transection. A recent study may explain this finding as it has shown that different sources of locomotion (controllers) are located in spinal cord rather than in the cortex of cat (Zelenin et al., 2011). After paralyzing spinal transection, efference copy cannot reach the brain (Orlovskii et al., 1999). However, the current study has demonstrated that different locomotive states (standing/walking) could still be decoded from these recordings and thus could be utilized for neurosprosthesis control.

The developed "Motolink" hardware utilizes this residual neural information to trigger stimulation signals for electrical activation of hindlimb muscles in order to mimic the walking function. Thus for the first time, a brain-machine-muscle interface was established for the restoration of hindlimb locomotion function in spinal rats.

As a significant outcome of this thesis, cortically controlled lower-limb neuroprosthesis is proposed for SCI paraplegics.

Future research directions

More work is needed to develop the concept of cortically triggering electrical stimulation for restoring lower-limb motor functions. A better understanding on spinal central pattern generator (CPG) in human will certainly help to design a better stimulation protocol. Moreover, bidirectional neural interface is one of the top priorities for the development of advanced neuroprosthetic devices. With sensory feedback it is expected that the recovery would be faster, better and permanent (Suminski et al., 2010). Intracortial Microstimulation (ICMS) has been explored for sensation feedback (O'Doherty et al., 2009). Since the SCI leaves healthy peripheral nerves intact along with spinal reflex loop circuits, one can alternatively use the dorsal root ganglions to record sensation and feed them into the ICMS system. This way we can use biological transduction of natural senses to produce electric impulses.

Balance is equally important function as walking, which requires extensive investigations. Apparently only one study in neuroprosthetics has been accomplished for balance decoding (Lebedev et al., 2011). Balance is an automatic body function, largely depends on the cerebellum and vestibular system. New neuroprosthetic approaches are needed for successfully interface these systems to restoring upright postures in paralysed patients. Alternatively, an artificial vestibular system can be developed by advanced electronic components to aid lower-limb neuroprosthesis. The knowledge gained from humanoid robots research (such as advanced algorithms) could be translated into these new neuroprosthetic systems.

Additionally, there are some very important bioengineering issues needed to be resolved. One of the most important issues is the biocompatibility of cortical and spinal electrodes and implants (Luo et al., 2007; Marin and Fernandez, 2010).

Compensating for the foreign body reaction, such as gliosis has been a big challenge towards the development of neural interface system. Researchers are working on this issue to develop advanced biomaterials that capable of high charge injection. Neural decoding is another engineering challenges needed to be solved (Nicolelis, 2007). Computation cost is too high, and it increases according to the increase of channel number. Though modern signal processors are mostly capable to achieve this demand, other drawbacks like the amount of heat dissipation, chip size, power requirements can limit the development of modern neuroprosthetic device.

There are some very important technical issues required to be addressed to develop successful neuroprosthetic system for real functional recovery for the paralysed. The first step of developing the multiple channels circuit to connect cortical motor neurons to a multichannel FES system has been achieved. But this needed to be extended more in channel numbers and in functionality. The decoding algorithm is very simple at the moment. New decoding algorithms are needed to be explored and adopted for better detection and decoding of cortical "intent" signals. Furthermore, to enable non-linear conversion of motor learning between the input and output functions of the "Motolink" neuroproshestic system smart machine-learning algorithms could be adopted. A multichannel, non-linear artificial intelligence neuroproshetic circuit may enable paralyzed patients to regain the ability to functionally move and walk. With the development of multichannel wireless neural signal transceiver, together with multichannel stimulation threads could be removed for better implant. This would further benefit the patient from avoiding the complications that may occur due to internal cablings. Large neuronal population recordings from parallel cortical channels of bilateral brain implants may help increase the decoding accuracy of cortical "intent" for the locomotion. The quality

and electrode numbers in the implant array needed to be improved and increased to acquire more accurate signals from the targeted area of the primary motor cortex for better and longer recordings. Neural networks control algorithm could also be explored for better decoding of neural signals.

The FES system utilized in the current study is only bilateral three channels intramuscular electrical stimulation. For functional walking, more stimulation channels are needed. Muscle fatigue is one of the major imitating factors of FES systems (Stokes and Cooper, 1989). Selecting appropriate stimulation parameters is the key of reducing muscle fatigue. Studies had shown that simply changing the frequency and pulse widths of the electrical stimulation may result substantial differences in muscle fatigues (Karu et al., 1995; Kesar and Binder-Macleod, 2006). However, it is still not possible to reduce the fatigue to zero with available FES systems (Graham et al., 2006). Various other methods such as fibre type conversion with chronic low frequency conditioning stimulation, sequential stimulation, optimization of stimulation parameters, and the uses of hybrid orthoses have been developed to minimize the fatigue due to stimulation (Cooper et al., 1989). Further research is needed to develop an optimum system that would provide prolonged stimulation without resulting major fatigue of the muscles.

REFERENCES

Agarwal S, Triolo RJ, Kobetic R, Miller M, Bieri C, Kukke S, Rohde L, Davis JA, Jr. (2003) Long-term user perceptions of an implanted neuroprosthesis for exercise, standing, and transfers after spinal cord injury. J Rehabil Res Dev 40:241-252.

Alam M, He J (2013) Cortically Controlled Electrical Stimulation for Locomotion of the Spinal Cord Injured. In: Converging Clinical and Engineering Research on Neurorehabilitation (Pons JL, Torricelli D, Pajaro M, eds), pp 35-40: Springer Berlin Heidelberg.

Anderson KD (2004) Targeting recovery: priorities of the spinal cord-injured population. J Neurotrauma 21:1371-1383.

Armstrong DM, Drew T (1984) Discharges of pyramidal tract and other motor cortical neurones during locomotion in the cat. J Physiol 346:471-495.

Bamford JA, Mushahwar VK (2011) Intraspinal microstimulation for the recovery of function following spinal cord injury. Prog Brain Res 194:227-239.

Behrman AL, Harkema SJ (2000) Locomotor Training After Human Spinal Cord Injury: A Series of Case Studies. Physical Therapy 80:688-700.

Behrman AL, Harkema SJ (2007) Physical Rehabilitation as an Agent for Recovery After Spinal Cord Injury. Physical Medicine and Rehabilitation Clinics of North America 18:183-202.

Beloozerova IN, Sirota MG (1993) The role of the motor cortex in the control of accuracy of locomotor movements in the cat. The Journal of Physiology 461:1-25.

Bernhard M, Gries A, Kremer P, Bottiger BW (2005) Spinal cord injury (SCI) - prehospital management. Resuscitation 66:127-139.

Bogdanov EI (2010) Spinal Injury. In: International Neurology, pp 652-654: Wiley-Blackwell.

Boord P, Barriskill A, Craig A, Nguyen H (2004) Brain-Computer Interface-FES Integration: Towards a Hands-free Neuroprosthesis Command System. Neuromodulation 7:267-276.

Branco F, Cardenas DD, Svircev JN (2007) Spinal Cord Injury: A Comprehensive Review. Physical Medicine and Rehabilitation Clinics of North America 18:651-679.

Braz GP, Russold M, Davis GM (2009) Functional electrical stimulation control of standing and stepping after spinal cord injury: a review of technical characteristics. Neuromodulation 12:180-190.

Carhart MR, Jiping H, Herman R, D'Luzansky S, Willis WT (2004) Epidural spinal-cord stimulation facilitates recovery of functional walking following incomplete spinal-cord injury. Neural Systems and Rehabilitation Engineering, IEEE Transactions on 12:32-42.

CDC (2010) Spinal Cord Injury (SCI): Fact Sheet In: http://www.cdc.gov/traumaticbraininjury/scifacts.html (Prevention CfDCa, ed). Atlanta, GA: US Government.

Chan CCH, Wong AWK, Ting K-H, Whitfield-Gabrieli S, He J, Lee TMC (2011) Cross auditory-spatial learning in early-blind individuals. Human Brain Mapping 33:2714-2727.

Chapin JK, Moxon KA, Markowitz RS, Nicolelis MAL (1999) Real-time control of a robot arm using simultaneously recorded neurons in the motor cortex. Nat Neurosci 2:664-670.

Chaplin E (1996) Functional neuromuscular stimulation for mobility in people with spinal cord injuries. The Parastep I System. J Spinal Cord Med 19:99-105.

Chiu WT, Lin HC, Lam C, Chu SF, Chiang YH, Tsai SH (2009) Review paper: epidemiology of traumatic spinal cord injury: comparisons between developed and developing countries. Asia Pac J Public Health 22:9-18.

Churchland MM, Cunningham JP, Kaufman MT, Foster JD, Nuyujukian P, Ryu SI, Shenoy KV (2012) Neural population dynamics during reaching. Nature advance online publication.

Cipriani C, Zaccone F, Micera S, Carrozza MC (2008) On the Shared Control of an EMG-Controlled Prosthetic Hand: Analysis of User–Prosthesis Interaction. Robotics, IEEE Transactions on 24:170-184.

Cogan SF (2008) Neural Stimulation and Recording Electrodes. Annual Review of Biomedical Engineering 10:275-309.

Collinger JL, Wodlinger B, Downey JE, Wang W, Tyler-Kabara EC, Weber DJ, McMorland AJC, Velliste M, Boninger ML, Schwartz AB (2012) High-performance neuroprosthetic control by an individual with tetraplegia. The Lancet 381:557-564.

Cooper RG, Stokes MJ, Gibson H, Edwards RH (1989) Review articles : Minimizing fatigue for functional electrical stimulation of muscle. Clinical Rehabilitation 3:333-340.

Courtine G, Gerasimenko Y, van den Brand R, Yew A, Musienko P, Zhong H, Song B, Ao Y, Ichiyama RM, Lavrov I, Roy RR, Sofroniew MV, Edgerton VR (2009) Transformation of nonfunctional spinal circuits into functional states after the loss of brain input. Nat Neurosci 12:1333-1342.

Cripps RA, Lee BB, Wing P, Weerts E, Mackay J, Brown D (2011) A global map for traumatic spinal cord injury epidemiology: towards a living data repository for injury prevention. Spinal Cord 49:493-501.

Crozier KS, Graziani V, Ditunno JF, Herbison GJ (1991) Spinal cord injury: prognosis for ambulation based on sensory examination in patients who are initially motor complete. Archives of Physical Medicine and Rehabilitation 72:119-121.

Davis JA, Jr., Triolo RJ, Uhlir J, Bieri C, Rohde L, Lissy D, Kukke S (2001) Preliminary performance of a surgically implanted neuroprosthesis for standing and transfers--where do we stand? J Rehabil Res Dev 38:609-617.

del-Ama AJ, Koutsou AD, Moreno JC, de-los-Reyes A, Gil-Agudo A, Pons JL (2012) Review of hybrid exoskeletons to restore gait following spinal cord injury. J Rehabil Res Dev 49:497-514.

Dethier J, Nuyujukian P, Ryu SI, Shenoy KV, Boahen K (2013) Design and validation of a real-time spiking-neural-network decoder for brain?□achine interfaces. Journal of Neural Engineering 10:036008.

Dietz V (2003) Spinal cord pattern generators for locomotion. Clinical Neurophysiology 114:1379-1389.

Dietz V, Fouad K, Bastiaanse CM (2001) Neuronal coordination of arm and leg movements during human locomotion. European Journal of Neuroscience 14:1906-1914.

Drew T (1988) Motor cortical cell discharge during voluntary gait modification. Brain Res 457:181-187.

Drew T (1991) Visuomotor coordination in locomotion. Curr Opin Neurobiol 1:652-657.

Drew T, Jiang W, Kably B, Lavoie S (1996) Role of the motor cortex in the control of visually triggered gait modifications. Can J Physiol Pharmacol 74:426-442.

Dromerick A, Lum P, Hidler J (2006) Activity-based therapies. NeuroRX 3:428-438.

Duysens J, Van de Crommert HWAA (1998) Neural control of locomotion; Part 1: The central pattern generator from cats to humans. Gait & Posture 7:131-141.

Edgerton VR, Roy RR (2009) Activity-dependent plasticity of spinal locomotion: implications for sensory processing. Exerc Sport Sci Rev 37:171-178.

Edgerton VR, Harkema S (2011) Epidural stimulation of the spinal cord in spinal cord injury: current status and future challenges. Expert Rev Neurother 11:1351-1353.

Edgerton VR, Roy RR (2012) A new age for rehabilitation. Eur J Phys Rehabil Med 48:99-109.

Eskandari P, Erfanian A (2008) Improving the performance of brain-computer interface through meditation practicing. In: Engineering in Medicine and Biology Society, 2008. EMBS 2008. 30th Annual International Conference of the IEEE, pp 662-665.

Ethier C, Oby ER, Bauman MJ, Miller LE (2012) Restoration of grasp following paralysis through brain-controlled stimulation of muscles. Nature 485:368-371.

Fifer MS, Acharya S, Benz HL, Mollazadeh M, Crone NE, Thakor NV (2011) Toward Electrocorticographic Control of a Dexterous Upper Limb Prosthesis: Building Brain-Machine Interfaces. Pulse, IEEE 3:38-42.

Fitzsimmons N, Lebedev M, Peikon I, Nicolelis MAL (2009) Extracting kinematic parameters for monkey bipedal walking from cortical neuronal ensemble activity. Frontiers in Integrative Neuroscience 3.

Fonoff ET, Pereira Jr JF, Camargo LV, Dale CS, Pagano RL, Ballester G, Teixeira MJ (2009) Functional mapping of the motor cortex of the rat using transdural electrical stimulation. Behavioural Brain Research 202:138-141.

Forrest GP, Smith TC, Triolo RJ, Gagnon J, DiRisio D, Miller ME, Rhodi L (2011) Use of the Case Western Reserve/Veterans Administration neuroprosthesis for exercise, standing and transfers by a paraplegic subject. Disabil Rehabil Assist Technol 7:340-344.

Fouad K, Pearson K (2004) Restoring walking after spinal cord injury. Progress in Neurobiology 73:107-126.

French DD, Campbell RR, Sabharwal S, Nelson AL, Palacios PA, Gavin-Dreschnack D (2007) Health care costs for patients with chronic spinal cord injury in the Veterans Health Administration. J Spinal Cord Med 30:477-481.

Freund P, Weiskopf N, Ward NS, Hutton C, Gall A, Ciccarelli O, Craggs M, Friston K, Thompson AJ (2011) Disability, atrophy and cortical reorganization following spinal cord injury. Brain 134:1610-1622.

Gerasimenko YP, Ichiyama RM, Lavrov IA, Courtine G, Cai L, Zhong H, Roy RR, Edgerton VR (2007) Epidural Spinal Cord Stimulation Plus Quipazine Administration Enable Stepping in Complete Spinal Adult Rats. Journal of Neurophysiology 98:2525-2536.

Gibson S, Judy JW, Markovic D (2008) Comparison of spike-sorting algorithms for future hardware implementation. In: Engineering in Medicine and Biology Society, 2008. EMBS 2008. 30th Annual International Conference of the IEEE, pp 5015-5020.

Graham GM, Thrasher TA, Popovic MR (2006) The effect of random modulation of functional electrical stimulation parameters on muscle fatigue. Neural Systems and Rehabilitation Engineering, IEEE Transactions on 14:38-45.

Graupe D (2002) An overview of the state of the art of noninvasive FES for independent ambulation by thoracic level paraplegics. Neurological Research 24:431-442.

Graupe D (2008) Transcutaneous FES for Ambulation: The parastep System. In: Neuroengineering (Dilorenzo DJ, Bronzino JD, eds). Boca Raton, FL: CRC Press.

Greene PJ, Granat MH (2003) A knee and ankle flexing hybrid orthosis for paraplegic ambulation. Medical Engineering & Physics 25:539-545.

Guiraud D, Stieglitz T, Koch KP, Divoux JL, Rabischong P (2006) An implantable neuroprosthesis for standing and walking in paraplegia: 5-year patient follow-up. J Neural Eng 3:268-275.

Harkema S, Behrman A, Barbeau H (2012) Evidence-based therapy for recovery of function after spinal cord injury. Handb Clin Neurol 109:259-274.

Harkema S, Gerasimenko Y, Hodes J, Burdick J, Angeli C, Chen Y, Ferreira C, Willhite A, Rejc E, Grossman RG, Edgerton VR (2011) Effect of epidural stimulation of the lumbosacral spinal cord on voluntary movement, standing, and assisted stepping after motor complete paraplegia: a case study. The Lancet 377:1938-1947.

He H, Jiping H, Herman R, Carhart MR (2006) Modulation effects of epidural spinal cord stimulation on muscle activities during walking. Neural Systems and Rehabilitation Engineering, IEEE Transactions on 14:14-23.

He J, Ma C, Herman R (2008) Engineering Neural Interfaces for Rehabilitation of Lower Limb Function in Spinal Cord Injured. Proceedings of the IEEE 96:1152-1166.

Hegarty D (2011) Spinal cord stimulation: the clinical application of new technology. Anesthesiol Res Pract 2012:375691.

Heuningen R, Goovaerts HG, Vries FR (1984) A low noise isolated amplifier system for electrophysiological measurements: basic considerations and design. Medical and Biological Engineering and Computing 22:77-85.

Hochberg LR, Serruya MD, Friehs GM, Mukand JA, Saleh M, Caplan AH, Branner A, Chen D, Penn RD, Donoghue JP (2006) Neuronal ensemble control of prosthetic devices by a human with tetraplegia. Nature 442:164-171.

Hochberg LR, Bacher D, Jarosiewicz B, Masse NY, Simeral JD, Vogel J, Haddadin S, Liu J, Cash SS, van der Smagt P, Donoghue JP (2012) Reach and grasp by people with tetraplegia using a neurally controlled robotic arm. Nature 485:372-375.

Holinski BJ, Mazurek KA, Everaert DG, Stein RB, Mushahwar VK (2011) Restoring stepping after spinal cord injury using intraspinal microstimulation and novel control strategies. In: Engineering in Medicine and Biology Society,EMBC, 2011 Annual International Conference of the IEEE, pp 5798-5801.

Hubli M, Dietz V (2013) The physiological basis of neurorehabilitation--locomotor training after spinal cord injury. J Neuroeng Rehabil 10:5.

Ichiyama RM, Gerasimenko YP, Zhong H, Roy RR, Edgerton VR (2005) Hindlimb stepping movements in complete spinal rats induced by epidural spinal cord stimulation. Neuroscience Letters 383:339-344.

Inman VT (1966) Human locomotion. Can Med Assoc J 94:1047-1054.

Isakov E, Douglas R, Berns P (1992) Ambulation using the reciprocating gait orthosis and functional electrical stimulation. Paraplegia 30:239-245.

Ivanenko YP, Cappellini G, Dominici N, Poppele RE, Lacquaniti F (2005) Coordination of Locomotion with Voluntary Movements in Humans. The Journal of Neuroscience 25:7238-7253.

Jackson A, Zimmermann JB (2012) Neural interfaces for the brain and spinal cord[mdash]restoring motor function. Nat Rev Neurol 8:690-699.

Jackson AB, Dijkers M, DeVivo MJ, Poczatek RB (2004) A demographic profile of new traumatic spinal cord injuries: Change and stability over 30 years. Archives of Physical Medicine and Rehabilitation 85:1740-1748.

Johnston TE, Betz RR, Smith BT, Mulcahey MJ (2003) Implanted functional electrical stimulation: an alternative for standing and walking in pediatric spinal cord injury. Spinal Cord 41:144-152.

Jung WG (2005) Op Amp applications handbook: Elsevier/Newnes.

Kakulas BA (1984) Pathology of spinal injuries. Cent Nerv Syst Trauma 1:117-129.

Kandel ER, Schwartz JH, Jessell TM (2000) Principles of Neural Science, 4 Edition: Elsevier.

Kantrowitz A (1960) Electronic physiological aids: A report of the Maimonides Hospital. Brooklyn, NY.

Karu ZZ, Durfee WK, Barzilai AM (1995) Reducing muscle fatigue in FES applications by stimulating with N-let pulse trains. Biomedical Engineering, IEEE Transactions on 42:809-817.

Kesar T, Binder-Macleod S (2006) Effect of frequency and pulse duration on human muscle fatigue during repetitive electrical stimulation. Experimental Physiology 91:967-976.

Kim S, Bhandari R, Klein M, Negi S, Rieth L, Tathireddy P, Toepper M, Oppermann H, Solzbacher F (2009) Integrated wireless neural interface based on the Utah electrode array. Biomedical Microdevices 11:453-466.

Kobetic R, To CS, Schnellenberger JR, Audu ML, Bulea TC, Gaudio R, Pinault G, Tashman S, Triolo RJ (2009) Development of hybrid orthosis for standing, walking, and stair climbing after spinal cord injury. J Rehabil Res Dev 46:447-462.

Krajl A, Bajd T, Turk R, Benko H (1986) Posture switching for prolonging functional electrical stimulation standing in paraplegic patients. Paraplegia 24:221-230.

Kralik JD, Dimitrov DF, Krupa DJ, Katz DB, Cohen D, Nicolelis MA (2001) Techniques for long-term multisite neuronal ensemble recordings in behaving animals. Methods 25:121-150.

Kralj A, Grobelnik S (1973) Functional electrical stimulation—A new hope for paraplegic patients? Bulletin of prosthetics research.

Kumar K, Toth C, Nath R, Laing P (1998) Epidural spinal cord stimulation for treatment of chronic pain? ome predictors of success. A 15-year experience. Surgical Neurology 50:110-121.

Lavrov I, Courtine G, Dy CJ, van den Brand R, Fong AJ, Gerasimenko Y, Zhong H, Roy RR, Edgerton VR (2008) Facilitation of Stepping with Epidural Stimulation in Spinal Rats: Role of Sensory Input. The Journal of Neuroscience 28:7774-7780.

Lebedev MA, Nicolelis MAL (2006) Brain-machine interfaces: past, present and future. Trends in Neurosciences 29:536-546.

Lebedev MA, Crist RE, Nicolelis MAL (2008) Building Brain-Machine Interfaces to Restore Neurological Functions.

Lebedev MA, Tate AJ, Hanson TL, Li Z, O'Doherty JE, Winans JA, Ifft PJ, Zhuang KZ, Fitzsimmons NA, Schwarz DA, Fuller AM, An JH, Nicolelis MAL (2011) Future developments in brain-machine interface research. Clinics 66:25-32.

Lee BB, Cripps RA, Fitzharris M, Wing PC (2013) The global map for traumatic spinal cord injury epidemiology: update 2011, global incidence rate. Spinal Cord.

Leuthardt EC, Schalk G, Moran D, Ojemann JG (2006) The emerging world of motor neuroprosthetics: a neurosurgical perspective. Neurosurgery 59:1-14; discussion 11-14.

Linderman MD, Santhanam G, Kemere CT, Gilja V, O'Driscoll S, Yu BM, Afshar A, Ryu SI, Shenoy KV, Meng TH (2008) Signal Processing Challenges for Neural Prostheses. Signal Processing Magazine, IEEE 25:18-28.

Lundy-Ekman L (2002) Neuroscience Fundamentals for Rehabilitation, 2 Edition: Elsevier Science.

Luo P, Xie G, Jiang Z (2007) The progress in researches on biocompatibility for direct brain-machine interface. Sheng Wu Yi Xue Gong Cheng Xue Za Zhi 24:1416-1418.

MacKay-Lyons M (2002) Central Pattern Generation of Locomotion: A Review of the Evidence. Physical Therapy 82:69-83.

Manohar A, Flint RD, Knudsen E, Moxon KA (2012) Decoding Hindlimb Movement for a Brain Machine Interface after a Complete Spinal Transection. PLoS One 7:e52173.

Marin C, Fernandez E (2010) Biocompatibility of intracortical microelectrodes: current status and future prospects. Front Neuroeng 3:8.

Matthew (2002) Spinal Cord Injury Facts & Statistics. In: Spinal Cord Injury Information Pages (Sci-info-pages, ed), pp http://www.sci-info-pages.com/facts.html. Michigan MCG Web Development, Inc.

Medina LE, Lebedev MA, O'Doherty JE, Nicolelis MAL (2012) Stochastic Facilitation of Artificial Tactile Sensation in Primates. The Journal of Neuroscience 32:14271-14275.

Miller S, van der Burg J, van der Meche FGA (1975) Coordination of movements of the hindlimbs and forelimbs in different forms of locomotion in normal and decerebrate cats. Brain Research 91:217-237.

Moritz CT, Fetz EE (2011) Volitional control of single cortical neurons in a brain-machine interface. Journal of Neural Engineering 8:025017.

Moritz CT, Perlmutter SI, Fetz EE (2008) Direct control of paralysed muscles by cortical neurons. Nature 456:639-642.

Motchenbacher CD, Connelly JA (1993) Low noise electronic system design: J. Wiley & Sons.

Mushahwar VK, Horch KW (2000) Selective activation of muscle groups in the feline hindlimb through electrical microstimulation of the ventral lumbo-sacral spinal cord. Rehabilitation Engineering, IEEE Transactions on 8:11-21.

Mushahwar VK, Saigal R (2002) Spinal cord stimulation for restoration of locomotion. In: Engineering in Medicine and Biology, 2002. 24th Annual Conference and the Annual Fall Meeting of the Biomedical Engineering Society EMBS/BMES Conference, 2002. Proceedings of the Second Joint, pp 2041-2042 vol.2043.

Mushahwar VK, Prochazka A (2004) spinal cord stimulation for restoring lower extremity function. In: Neuroprosthetics: theory and practice (Horsch KW, Dhillon GS, eds): World Scientific.

Mushahwar VK, Jacobs PL, Normann RA, Triolo RJ, Kleitman N (2007) New functional electrical stimulation approaches to standing and walking. Journal of Neural Engineering 4:S181.

Musienko P, van den Brand R, Marzendorfer O, Roy RR, Gerasimenko Y, Edgerton VR, Courtine G (2011) Controlling Specific Locomotor Behaviors through Multidimensional Monoaminergic Modulation of Spinal Circuitries. The Journal of Neuroscience 31:9264-9278.

Neafsey EJ, Bold EL, Haas G, Hurley-Gius KM, Quirk G, Sievert CF, Terreberry RR (1986) The organization of the rat motor cortex: a microstimulation mapping study. Brain Res 396:77-96.

NeuRA (2009) Nerve & Spinal Cord Injury. In: (Australia NR, ed), pp http://www.neura.edu.au/health/nerve-and-spinal-cord-injury. Randwick, NSW: Neuroscience Research Australia.

Nicolelis MAL (2003) Brain-machine interfaces to restore motor function and probe neural circuits. Nat Rev Neurosci 4:417-422.

Nicolelis MAL (2007) Methods for Neural Ensemble Recordings, Second Edition: Taylor & Francis.

Nishimura Y, Perlmutter SI, Fetz EE (2013) Restoration of upper limb movement via artificial corticospinal and musculospinal connections in a monkey with spinal cord injury. Frontiers in Neural Circuits 7.

Noonan VK, Kwon BK, Soril L, Fehlings MG, Hurlbert RJ, Townson A, Johnson M, Dvorak MF (2012) The Rick Hansen Spinal Cord Injury Registry (RHSCIR): a national patient-registry. Spinal Cord 50:22-27.

O'Connor PJ (2004) Prevalence of spinal cord injury in Australia. Spinal Cord 43:42-46.

O'Doherty JE, Lebedev MA, Zheng L, Nicolelis MAL (2012) Virtual Active Touch Using Randomly Patterned Intracortical Microstimulation. Neural Systems and Rehabilitation Engineering, IEEE Transactions on 20:85-93.

O'Doherty JE, Lebedev MA, Hanson TL, Fitzsimmons NA, Nicolelis MA (2009) A brain-machine interface instructed by direct intracortical microstimulation. Front Integr Neurosci 3:20.

Orlovskii GGN, Deliagina TG, Grillner S (1999) Neuronal Control of Locomotion: From Mollusc to Man: Oxford University Press.

Pedotti A, Ferrarin M, Communities CotE (1992) Restoration of Walking for Paraplegics: Recent Advancements and Trends: Pro Juventute.

Pfurtscheller G, Leeb R, Keinrath C, Friedman D, Neuper C, Guger C, Slater M (2006) Walking from thought. Brain Research 1071:145-152.

Pikov V (2008) Clinical Applications of Intraspinal Microstimulation. Proceedings of the IEEE 96.

Qiu J (2009) China Spinal Cord Injury Network: changes from within. The Lancet Neurology 8:606-607.

Quintero HA, Farris RJ, Durfee WK, Goldfarb M (2010) Feasibility of a hybrid-FES system for gait restoration in paraplegics. Conf Proc IEEE Eng Med Biol Soc 2010:483-486.

Ragnarsson KT (1988) Physiologic effects of functional electrical stimulation-induced exercises in spinal cord-injured individuals. Clin Orthop Relat Res:53-63.

Rossignol S, Frigon A (2011) Recovery of Locomotion After Spinal Cord Injury: Some Facts and Mechanisms. Annual Review of Neuroscience 34:413-440.

Rouse AG, Stanslaski SR, Cong P, Jensen RM, Afshar P, Ullestad D, Gupta R, Molnar GF, Moran DW, Denison TJ (2011) A chronic generalized bi-directional brain-machine interface. Journal of Neural Engineering 8:036018.

Sadowsky CL, McDonald JW (2009) Activity-based restorative therapies: concepts and applications in spinal cord injury-related neurorehabilitation. Dev Disabil Res Rev 15:112-116.

SCI-recovery (2013) Spinal Cord Injuries. In, pp http://www.sci-recovery.org/sci.htm.

Scott SH (2008) Cortical-based neuroprosthetics: when less may be more. Nat Neurosci 11:1245-1246.

SIA (2010) Facts & statistics. In: Facts & statistics (Association SI, ed), pp http://www.spinal.com.au/information/facts-statistics/. Woolloongabba, QLD: National Disability Services

Stokes M, Cooper R (1989) Muscle fatigue as a limiting factor in functional electrical stimulation: A review. Physiotherapy Theory and Practice 5:83-90.

Suminski AJ, Tkach DC, Fagg AH, Hatsopoulos NG (2010) Incorporating Feedback from Multiple Sensory Modalities Enhances Brain-machine Interface Control. The Journal of Neuroscience 30:16777-16787.

Thuret S, Moon LDF, Gage FH (2006) Therapeutic interventions after spinal cord injury. Nat Rev Neurosci 7:628-643.

Turner DA, Patil PG, Nicolelis MAL (2008) Conceptual and Technical Approaches to Human Neural Ensemble Recordings.

Van de Crommert HWAA, Mulder T, Duysens J (1998) Neural control of locomotion: sensory control of the central pattern generator and its relation to treadmill training. Gait & Posture 7:251-263.

van den Berg ME, Castellote JM, de Pedro-Cuesta J, Mahillo-Fernandez I (2010) Survival after spinal cord injury: a systematic review. J Neurotrauma 27:1517-1528.

van den Brand R, Heutschi J, Barraud Q, DiGiovanna J, Bartholdi K, Huerlimann M, Friedli L, Vollenweider I, Moraud EM, Duis S, Dominici N, Micera S, Musienko P, Courtine G (2012) Restoring Voluntary Control of Locomotion after Paralyzing Spinal Cord Injury. Science 336:1182-1185.

Wahnoun R, He J, Tillery SIH (2006) Selection and parameterization of cortical neurons for neuroprosthetic control. Journal of Neural Engineering 3:162.

Wang W, Collinger JL, Degenhart AD, Tyler-Kabara EC, Schwartz AB, Moran DW, Weber DJ, Wodlinger B, Vinjamuri RK, Ashmore RC, Kelly JW, Boninger ML (2013) An electrocorticographic brain interface in an individual with tetraplegia. PLoS One 8:e55344.

Waters RL, Adkins RH, Yakura JS (1991) Definition of complete spinal cord injury. Paraplegia 29:573-581.

Wattanapanitch W, Fee M, Sarpeshkar R (2007) An Energy-Efficient Micropower Neural Recording Amplifier. Biomedical Circuits and Systems, IEEE Transactions on 1:136-147.

Weiguo S, Ramakrishnan A, Udoekwere UI, Giszter SF (2009) Multiple Types of Movement-Related Information Encoded in Hindlimb/Trunk Cortex in Rats

and Potentially Available for Brain–Machine Interface Controls. Biomedical Engineering, IEEE Transactions on 56:2712-2716.

Wessels M, Lucas C, Eriks I, de Groot S (2010) Body weight-supported gait training for restoration of walking in people with an incomplete spinal cord injury: a systematic review. J Rehabil Med 42:513-519.

WHO (2011) World report on disability. In: World report on disability (Organization WH), p http://whqlibdoc.who.int/publications/2011/9789240685215_eng.pdf. Geneva: World Helth Organization.

Wyndaele M, Wyndaele JJ (2006) Incidence, prevalence and epidemiology of spinal cord injury: what learns a worldwide literature survey? Spinal Cord 44:523-529.

Xiao-qin L, Xing W, Chang L (2011) SPKtool: An open source toolbox for electrophysiological data processing. In: Biomedical Engineering and Informatics (BMEI), 2011 4th International Conference on, pp 854-857.

Xie M, Xiong Y, Xiong C, Liu H, Hu Z, Zhang D, Liu G, Huan G, Liu J, Zhu X (2009) A Hybrid FES Rehabilitation System Based on CPG and BCI Technology for Locomotion: A Preliminary Study. In: Intelligent Robotics and Applications, pp 1073-1084: Springer Berlin Heidelberg.

Ying Z, Roy RR, Edgerton VR, Gomez-Pinilla F (2005) Exercise restores levels of neurotrophins and synaptic plasticity following spinal cord injury. Experimental Neurology 193:411-419.

Yu X-J, Xu X-X, He S, He J (2009) Change detection by thalamic reticular neurons. Nat Neurosci 12:1165-1170.

Zacksenhouse M, Nemets S (2008) Strategies for Neural Ensemble Data Analysis for Brain-Machine Interface (BMI) Applications.

Zelenin PV, Deliagina TG, Orlovsky GN, Karayannidou A, Dasgupta NM, Sirota MG, Beloozerova IN (2011) Contribution of Different Limb Controllers to Modulation of Motor Cortex Neurons during Locomotion. The Journal of Neuroscience 31:4636-4649.

Zhang F, Aghagolzadeh M, Oweiss K (2012) A Fully Implantable, Programmable and Multimodal Neuroprocessor for Wireless, Cortically Controlled Brain-Machine Interface Applications. Journal of Signal Processing Systems 69:351-361.